Assessment of the potential for underground hydrogen storage in salt domes

Leszek Lankof *
Mineral and Energy Economy Research Institute of the Polish Academy of Sciences,
Wybickiego 7A, 31-261, Krakow, Poland

Kazimierz Urbańczyk
Ubroservice, ul. Lea 149A, 30-133 Krakow, Poland

Radosław Tarkowski
Mineral and Energy Economy Research Institute of the Polish Academy of Sciences,
Wybickiego 7A, 31-261, Krakow, Poland

Abstract

The study concerns the critical issue of large-scale hydrogen storage in salt domes. The article aims to present the methodology for the hydrogen storage potential assessment for salt domes. The method considers the size of storage caverns, their depth, the influence of convergence, and the geological structure of the selected salt domes. Statistical analysis of data from the underground cavern storage facility in the Mogilno salt dome allows determining the probability of constructing a salt cavern of a specific volume and depth in the selected salt domes. Estimates based on the developed methodology indicate that the average hydrogen storage potential for the analyzed salt domes ranges from 125.7 TWh_t after the first filling to 83.8 TWh_t after 30 years of operation. The maximum storage potential ranges from 178 to 155 TWh_t, respectively. In the case of the largest analyzed salt dome, where one may construct salt caverns at a depth that ensures moderate convergence, the storage potential amounts to 34.3 TWh_t after first filling. The presented methodology is the next phase of the research, which refines the previous estimates, allowing for more accurate forecasts of rock salt deposit capacity in terms of hydrogen storage. The presented problems are of interest to countries considering large-scale hydrogen storage, geological survey organizations, companies producing electricity from renewables, and petrochemical companies considering underground hydrogen storage in salt caverns.

* Corresponding author: E-mail address: lankof@min-pan.krakow.pl (L.Lankof).

Highlights

- The methodology allows determining the potential for hydrogen storage in salt domes
- The cavern volume, depth, and convergence has a significant impact on its capacity
- The complex geological structure of salt domes diminishes their storage potential
- The storage potential in salt domes significantly exceeds current demand

Keywords:

large scale hydrogen storage, salt cavern, salt dome, cavern capacity, convergence, storage potential, renewable energy sources

Word Count: 7542

Nomenclature

A – surface area of anticlinal structures at a depth of the salt mirror [km^2]
A_1 – constant coefficient in the convergence formula [‰/year]
C – salt dome storage capacity per area [thousand Nm^3/m^2]
f – coefficient of the hydrogen-filled cavern volume to its total volume (assumed as 0.8)
g – standard gravity [m/s^2]
g_f – allowable gradient of the maximum hydrogen storage pressure [MPa/m]
g_{pmin} – minimum storage pressure gradient [MPa/m]
g_T – geothermal gradient [K/m]
H – cavern height including the neck and excluding the sump and the residual brine [m]
h_0 – maximum depth of the center of a salt cavern that can be safely emptied [m]
h_{cc} – cavern center depth [m]
h_{cem} – depth of the last cemented casing shoe [m]
h_{top} – the salt mirror depth [m]
$\bar{k}$ – average annual convergence [‰]
$k(p)$ – the rate of cavern relative convergence at hydrogen pressure p [‰/year]
m_{Nm3} – the amount of hydrogen in the cavern [Nm^3]
n – exponent in the convergence formula [–]
p – cavern pressure [MPa]
P – salt dome surface area at a depth of the salt mirror [km^2]
p_∞ – primary lithostatic pressure [MPa]
p_{cem} – pressure at the last cemented casing shoe depth [MPa]
p_h – brine head pressure [MPa]
p_{max} – maximum storage pressure [MPa]
p_{min} – minimum storage pressure [MPa]
Q_1 – constant coefficient in the convergence formula, the equivalent of activation energy [J/kg]
R – gas constant [J/kgK]
S – surface area assigned to a single cavern in a triangular grid [m^2]
t – operation time [years]
T – hydrogen temperature in the salt cavern [K]

T_m – rock mass temperature according to the geothermal gradient [K]
T_{m0} – rock mass temperature on the surface [K]
V – geometric volume of the cavern [m^3]
Z – hydrogen compressibility coefficient [-]
Δm_{Nm3} – stored hydrogen mass increase with a pressure change by Δp [Nm^3]
Δp – cavern pressure working range
Δp_{hydr} – hydraulic resistance increased by the brine pressure on the head [MPa]
Δt_{in} – the period when cavern is filling to the maximum pressure [days]
Δt_{max} – the period when cavern is under the maximum pressure [days]
Δt_{min} – the period when cavern is under the minimum pressure [days]
Δt_{exp} – the period when cavern is exploited to the minimum pressure [days]

Greek symbols
μ – expected value
ρ_b – brine density [kg/m^3]
ρ_H – hydrogen density under standard conditions [kg/m^3]
ρ_o – density of overburden rocks [kg/m^3]
ρ_s – density of rock salt, [kg/m^3]
σ_0 – the dimensional constant in the formula for convergence, σ_0 =1MPa

Abbreviations
bgl – *below ground level*
CAES – compressed air energy storage
CGSF – cavern gas storage facility
IRES – intermittent renewable energy sources
NG – natural gas
RES – renewable energy sources
UGS – underground gas storage
UHS – underground hydrogen storage

Statistical nomenclature
a, b, c, d – *trapezoidal distribution parameters*
f(h) – *trapezoidal distribution of caverns depths*
f(V) – *triangular distribution of caverns volumes*
s(h) – *the probability function of caverns depth in the Mogilno salt dome*
V_0, V_1, V_2 – *triangular distribution parameters*
ϑ – *unit step function of salt cavern depth*
μ – *expected value corresponding to the caverns' average depth or volume value*
σ – *standard deviation from the caverns' average depth or volume value*

1. Introduction

Probably renewable energy, based on wind and solar power plants, becomes a significant energy source shortly. In that case, storage systems of multi-megawatt capacity will be necessary [1–3]. Underground storage of large quantities of hydrogen produced by electrolysis of water using off-peak power may prove an economically viable solution for different time scales. Salt caverns are considered a favorable option for storing large amounts of hydrogen [4–6].

Hydrogen offers the solution sought for the decarbonization of industrial processes and those sectors of the economy where reducing carbon dioxide emissions is difficult to achieve [7]. Today, still partially, but in the 2050 perspective, it should replace natural gas (NG) in the chemical industry, metallurgy, transport, and in the long-term, aviation and maritime sectors (COM/2020/301). The technology of hydrogen production by electrolysis has been intensively developed in recent years. One of its advantages is virtually unlimited availability of the raw material, water. However, the condition for its widespread use will be the availability of significant resources of cheap energy from renewable energy sources (RES) [8]. Moreover, with the growing role of hydrogen produced using intermittent renewable energy sources (IRES), the possibility of large-scale storage will be necessary to consider.

1.1. Literature review

Porous geological structures and caverns constructed in rock salt formations [9–11] are considered for underground hydrogen storage (UHS). Currently, salt caverns are typically regarded as the best for UHS [12–14]. Rock salt deposits commonly occur worldwide as bedded formations or structures uplifted by halotectonic processes (Fig. 1). There are numerous hydrocarbon storage facilities in both types of deposits [15–17].

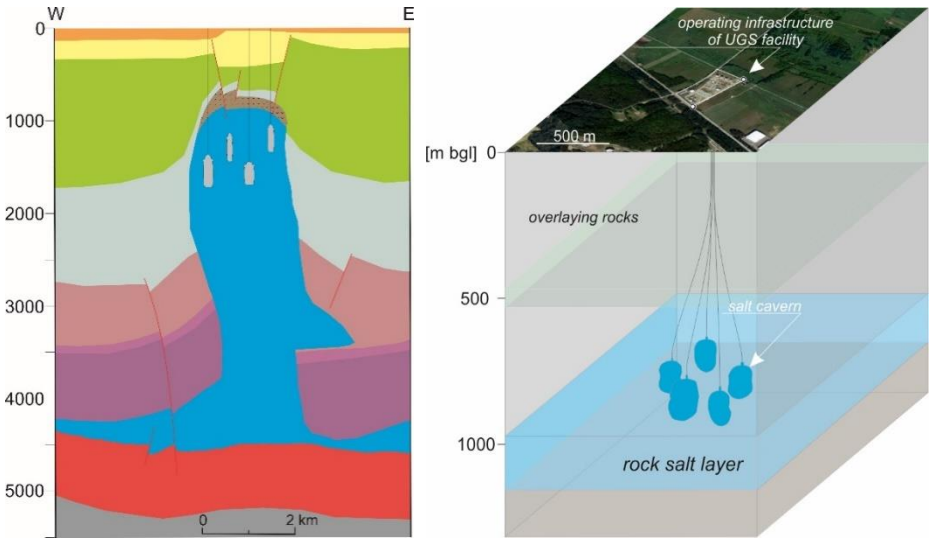

Fig. 1 – Salt caverns in salt domes and bedded salt formations based on [18]

Low porosity and permeability, chemical inertness, and a common occurrence in the form of thick layers and salt domes make rock salt very suitable for large-scale hydrogen storage [14,19,20]. In addition, the specific properties of rock salt ensure the long-term stability and tightness of storage facilities [21–23]. Furthermore, other positive features of rock salt in terms of underground storage include the large capacity of salt caverns, small surface area for a storage facility, flexible operation with multiple injections and withdrawals cycles per year, and storage safety emphasized by [24,25].

Hydrogen behavior is more complex than expected because of its physical and chemical properties and the interaction with the environment during storage [11,25]. Practical experience with hydrogen storage is still limited. There are only four active storage facilities in rock salt for the petrochemical industry: one in Teesside in the UK and three in the US, operated by Praxair, Conoco Philips, and Air Liquide [13,26,27].

Assessment of the potential for hydrogen storage in salt caverns. The feasibility of hydrogen storage in salt caverns has recently been assessed in several countries [17,28,29]. Already Crotogino and Huebner [30] have pointed to the use of salt caverns for large-scale underground storage of renewable energy through hydrogen production by electrolysis. The occurrence of thick, relatively pure rock salt layers at a sufficient depth, preferably 1000 – 2000 m bgl (below ground level), access to fresh water for salt leaching, and economically and ecologically acceptable means of brine disposal are indicated by Matos et al. [20] as essential conditions for site selection for the underground cavern storage facilities. While assessing the engineering potential for hydrogen storage, Chapman et al. [31] emphasized that the costs of hydrogen production, storage, and transport are significant obstacles to the launch of the

hydrogen economy. Executive Summary of the HyUnder project [32] presents the potential, stakeholders, and relevant business cases for the large-scale and long-term UHS produced from IRES in six European countries, pointing to the northern parts of Germany and the Netherlands as particularly promising. The Spanish case study of the HyUnder project evaluated the potential of large-scale UHS in salt caverns [33]. Caglayan et al. [34] presented the technical potential for hydrogen storage in bedded salt formations and salt domes in Europe. The total onshore and offshore technical storage potential was estimated at 84.8 $PWhH_2$. The highest national storage potential of 9.4 $PWhH_2$ was reported for Germany. Mouli-Castillo et al. [35] presented a method of assessing geological storage capacity concerning the seasonal heating demand. Their calculations showed that in the case of Great Britain, the geological storage potential exceeds the heating demand. Considering the economic, technical, and environmental factors of large-scale hydrogen storage, Stone et al. [36] identified several potential sites for hydrogen storage in the UK, which would help compensate for fluctuations in hydrogen demand and provide a strategic reserve. Juez-Larré et al. [37] analyzed the onshore and offshore hydrogen storage potential in the Netherlands and estimated the candidate fields storage capacity for NG and hydrogen. They also indicated the existing limitations resulting from the rate of cavern leaching, brine management, and surface subsidence above salt caverns.

Carneiro et al. [38] evaluated the occurrence of geological formations in mainland Portugal suitable for large-scale energy storage, identifying the most significant potential for compressed air energy storage (CAES) and underground gas storage (UGS) in salt formations and existing salt caverns. Ozarslan [39] assessed the possibility of using a salt cavern in Turkey to store hydrogen produced from solar energy. A preliminary assessment of underground storage of hydrogen produced from excess electricity in porous media and salt caverns in Ontario (Canada) was presented by Lemieux et al. [40]. Qiu et al. [41] analyzed depleted hydrocarbon reservoirs and salt caverns in an integrated energy system based on potential scenarios for UHS in different regions in China.

Czapowski [42] discussed the geological conditions and prospects for the location of hydrogen storage caverns in the Permian rock salt deposits in Poland, while Tarkowski and Czapowski [14] identified seven salt domes not disturbed by mining activity in Poland as the most promising for UHS. Ślizowski, Urbańczyk et al. [43] determined the capacity of NG and hydrogen storage caverns depending on the geological and mining conditions in rock salt deposits in the northern part of Poland. They presented maps showing the amount of energy that may be stored per area. Lankof and Tarkowski [44] assessed the potential of UHS in bedded rock salt formations in the southwestern region of Poland, stating that

underground storage of this gas requires the evaluation of the underground storage potential on a regional, national, and local scale. For the selected area, based on maps of the energy value of stored hydrogen, they presented a detailed assessment of the storage capacity for a single cavern and a cavern field.

The size and shape of salt caverns. The dimensions and shapes of salt caverns may vary, depending on needs, rock salt properties, and geological and mining conditions. Wang et al. [45] proposed a model for designing the shape and dimensions of a cavern, indicating that the maximum gas pressure determines the shape and dimensions of the lower part of the cavern, while the minimum gas pressure determines the shape and dimensions of its upper part. Yee [46] presented a leaching program for an existing salt dome storage cavern, resulting in increased storage capacity. Cyran [47] discussed the influence of geological factors on the salt cavern shape, emphasizing that the rational design of the cavern depends on the mechanical parameters of rock salt and other evaporite rocks, stability conditions, safety requirements, and the stored medium. The results of shape modeling for the optimization of salt cavern volume, including hydrogen, were also discussed by Cyran and Kowalski [48].

Storage Pressure. Storage pressure **i**s an important parameter that determines the efficiency and safety of UHS in salt caverns. Ślizowski et al. [49] emphasize that exceeding the allowable storage pressure gradient may lose cavern integrity. Bérest et al. [50] presented the results of tests on the maximum allowable pressures in salt caverns to prevent leakages. Wang et al. [51], considering the possibility of increasing the salt cavern capacity, analyzed the maximum allowable gas pressure based on hydraulic fracturing tests. Ślizowski et al. [52] presented preliminary results of in-situ fracturing tests of bedded salt formations in SW Poland. The obtained results indicate that the design of a salt cavern for hydrogen storage cannot assume the same maximum pressure gradient of $18.08 \cdot 10^{-3}$ MPa/m as is accepted for NG in the Mogilno and Kosakowo cavern gas storage facilities (CGSF). It is expected that this value will need to be reduced to the range of $15–16 \cdot 10^{-3}$ MPa/m, which should be further verified by micro fracturing tests in the borehole.

Rock salt properties that affect their behavior during hydrogen storage. During construction and operation, salt caverns are subjected to various load conditions. The mechanical and thermomechanical responses of rock salt during all stages of the cavern life, such as the leaching phase [53], first filling, and operation, are frequently discussed [54–56]. Passaris et al. [57] presented the analysis results to evaluate rock salt creep parameters to understand better the conditions ensuring the long-term cavern stability.

Böttcher et al. [58] present the results of a thermomechanical study of salt caverns designed for short-term cyclic hydrogen storage. They indicate that large temperature amplitudes in the working gas

may lead to tensile stresses at the cavern boundary. In turn, reducing the frequency of cyclic gas injection may be a way to reduce temperature fluctuations.

Khaledi et al. [21] discussed the stability and usefulness of underground storage caverns in rock salt subjected to cyclic mechanical loading. The rheological properties of rock salt are of great importance for the capacity of salt caverns. The significance of the tightness of rock salt due to its permeability is also emphasized [59–63]. Abuaisha and Billiotte [64] indicated that hydrogen losses in salt caverns due to diffusion, even with conservative assumptions, are very negligible.

The results of laboratory tests of geochemical reactivity of dissolved hydrogen with clay minerals of rock salt interlayers show [65] that the hydrogen diffusivity may cause several problems and limitations, affecting storage in salt caverns. The potential risk of H_2S generation and release in salt cavern storage was discussed by [66] as a factor that threatens the safe storage of hydrogen. Schlichtenmayer et al. [67] investigated the permeability of rock salt samples. They observed no differences in the permeability of the rock salt for experiments conducted with (NG), hydrogen, and air, indicating the suitability of salt caverns for high-pressure hydrogen storage.

1.2. Research objective

The problem presented in this article concerns a systematic approach to assessing the potential for UHS in specific, commonly occurring structures of rock salt deposits such as salt domes. Estimations of hydrogen storage capacity in rock salt deposits are increasingly carried out on the continental, regional, and country scales. They present initial capacity estimates and are based on general assumptions, using publicly available data, providing a starting point for the more detailed capacity estimates, which requires a different approach, both for bedded salt formations and salt domes.

Lankof and Tarkowski [44] presented the methodological basis for assessing the hydrogen storage capacity of salt caverns. However, they mainly focused on bedded salt formations. Estimating the storage potential of salt domes requires a different approach due to their specific geological structure.

Therefore, continuing the previous research, a methodological basis for a detailed assessment of hydrogen storage potential for salt domes was developed. Using the proposed methodology, the hydrogen storage potential for the selected salt domes in Poland was assessed.

The parameters of the hydrogen storage in salt caverns will ultimately depend on the investor's needs and will require detailed analyzes at the cavern design stage. The methodology may help decide whether and where to invest and what storage capacity to expect.

2. Methodology for assessing the potential for underground hydrogen storage in salt domes

Storage caverns in rock salt deposits are usually constructed in the 500 – 1800 m bgl depth range [16]. Taking the complex geological structure of salt domes into account, only the salt domes in which the top of the rock salt (salt mirror) occurs not deeper than 1500 m bgl were taken for further consideration. That increases the chances of encountering a suitable pure rock salt layer in an additional 300 m depth range (1500-1800 m bgl). The adopted criterion allows for the selection of 7 salt domes for further analysis. Fig. 2 and Table 1. present the selected salt domes.

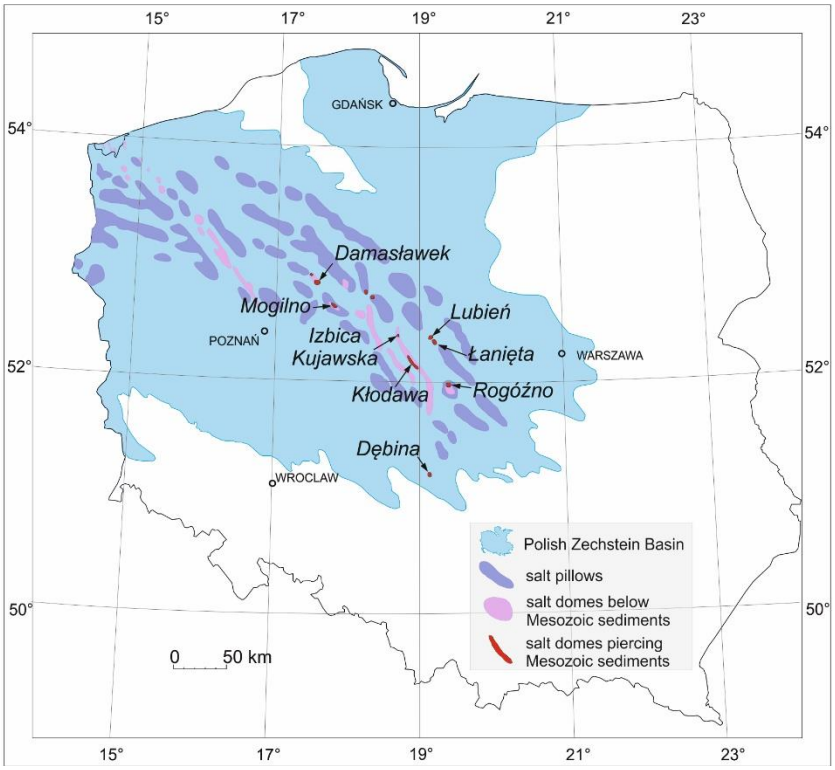

Fig. 2 – Map of the Polish Zechstein Basin with salt domes selected for the hydrogen storage potential assessment.

Table 1. The selected salt domes for the assessment of hydrogen storage capacity

No.	Salt dome	Salt dome surface area [km^2]	Salt mirror depth [m bgl]
1.	Damasławek	13.0	446.0-497.0
2.	Dębina	0.5	169.3-215.0
3.	Izbica	4.0	327.7-354.5
4.	Kłodawa (beyond mining area)	21.0	227.5-532.2
5.	Lubień	5.9	303.0-441.6
6.	Łanięta	9.5	235.4-303.8
7.	Rogóźno	21.0	320.9-372.8

The methodology determining the storage potential of the selected salt domes involves the following steps:

- the assessment of the maximum salt cavern height depending on its depth,
- the evaluation of the optimum depth for the storage cavern,
- the evaluation of the convergence impact on the capacity of hydrogen storage caverns,
- the statistical analysis aimed at determining the distribution and the probability density function of storage caverns depth and volume in the CGSF Mogilno,
- determination of individual A/P coefficients for each analyzed salt dome. A/P coefficient is the ratio of the surface area of the anticlinal structures including rock salt (A) at a depth of the salt mirror, to the surface area of the analyzed salt dome at the same depth (P),
- determination of parameters of the statistical distributions of a storage cavern depth and volume in the selected salt domes based on the statistical analysis of the CGSF Mogilno data and the individual A/P coefficients,
- calculations of the storage potential of the selected salt domes considering the results of the statistical analysis.

The assessment of the size of the hydrogen storage cavern was aimed at determining its maximum safe size, not affecting its stability. Evaluating the optimum cavern depth allows us to adjust the expected value of the cavern depth determined by statistical analysis, to improve cavern storage capacity. The analysis of the salt caverns convergence assumed two variants of the convergence rate: optimistic and pessimistic, determined in the previous research on rheological properties of rock salts from Polish salt domes [68]. The analysis was aimed to determine the potential storage capacity loss depending on the cavern depth and the assumed convergence variant.

Statistical analysis of data concerning salt caverns depth and volume in the CGSF Mogilno allowed us to determine the expected values of caverns depths and volumes. The generalization of the statistical parameters to the other salt domes was carried out by determining the A/P coefficients for each salt dome. The calculations of the potential of each selected salt dome take the expected values for the cavern depth and volume and A/P coefficients into account. The interaction between caverns should be insignificant, so to ensure caverns' stability, the distance of 250 m between salt caverns axes was assumed in the calculations. Different criteria, such as dilation criterion or volume loss rates, determine dimensions of safety pillars between salt caverns. Zapf [69] recommends remaining the safety pillar with a horizontal dimension of 1.8 to 2.2 times the average diameter of two neighbor caverns. In the case of the Jintan salt deposit in China, Wang T. et al. [70] recommend leaving the safety pillar 2.0 times larger than the cavern's diameter, based on detailed geomechanical analysis. In Polish conditions, the distance of 250 m between salt cavern axes was assumed, taking into account that the geological structure of the salt domes limits the size of storage caverns. Assuming the safety pillar dimensions equal 1.8 - 2.2 of cavern diameter according to Zapf [69] and 250 m distance between cavern axes, one may construct caverns with a maximum diameter from 78 to 89 m. This assumption made it possible to calculate the average and maximum storage potential of the selected salt domes and the storage potential per area. Calculations assumed the pessimistic variant of convergence to illustrate the changes in storage capacity over time. The storage potential is expressed as the volume [Nm^3] and stored hydrogen energy [TWh_t].

3. The theoretical background of assessing the storage potential of salt domes

3.1. Caverns height in the salt dome

Two aspects are crucial in terms of the size of a cavern in salt domes: the geological structure of the salt dome, and the geomechanical stability and integrity of the caverns. The upper limit of the cavern height can be obtained as follows:

The safety condition which must be met to ensure the integrity of the rock mass is defined by the formula (1).

$$p_{cem} \leq h_{cem} \cdot g_f \tag{1}$$

where p_{cem} represents the pressure at the last cemented casing shoe depth, h_{cem} the depth of the last cemented casing shoe, and g_f allowable gradient of the maximum hydrogen storage pressure (0.016 MPa/m), adopted after Ślizowski et al. [52].

The critical value of p_{cem} is determined at the end of the first filing of the cavern with hydrogen. The pressure at the last cemented casing shoe's depth corresponds to the brine's pressure in the casing string minus the pressure of the hydrogen column in the cavern plus the hydraulic resistance of the brine flow. The formula (2) gives the pressure at the last casing shoe depth:

$$p_{cem} = \rho_b g(h_{cem} + H) - \rho_H g H + \Delta p_{hydr} + p_h \quad (2)$$

where ρ_b is brine density, g standard gravity, ρ_H hydrogen density, H cavern height including the neck and excluding the sump and the residual brine, p_h brine head pressure, and Δp_{hydr} hydraulic resistance of the brine flow.

Taking into account the low density of hydrogen and the low hydraulic flow resistance, these two terms can be neglected and the limitation of cavern height can be safely approximated by the formula (3):

$$H \leq h_{cem}\left(\frac{g_f}{g\rho_b} - 1\right) - \frac{p_h}{g\rho_b} \quad (3)$$

The previous calculations [68] indicate that the differences between the maximum cavern heights approximated by the formula used and the detailed estimates are understated approx. 3.5% at a depth of 500 m, by approx. 11.5% at a depth of 1200 m, and 19.0% at 1800 m.Fig. 3 shows the maximum height of the hydrogen storage cavern depending on the depth of the last cemented casing shoe. The maximum height of the hydrogen storage cavern is about 30-40% lower than that of NG caverns. This difference is due to the g_f values for hydrogen and NG assuming a conservative approach of calculations presented by authors.

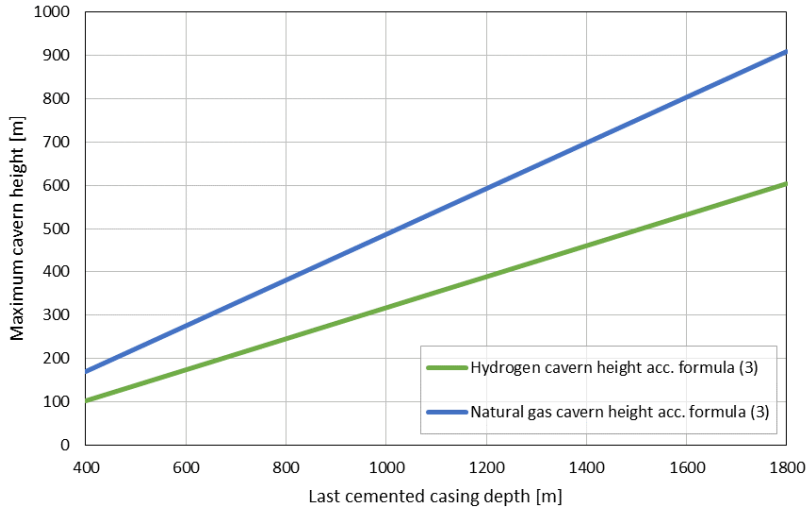

Fig. 3 – Maximum height of hydrogen storage caverns depending on depth and calculation method.

The estimates show that with conservative assumptions, at a depth of 1000 m bgl, it is possible to construct caverns with a maximum height of 300 m, providing a large storage capacity. However, there is a low probability of leaching caverns with the maximum height resulting from these estimates, considering the geological structure of Polish salt domes.

3.2. Depth of salt cavern

The depth that allows the largest amount of hydrogen to be stored was assumed to be the most favorable for the storage cavern. The amount of hydrogen which may be stored in one cubic meter of cavern defines the formula (4):

$$\frac{\Delta m_{Nm^3}}{1m^3} = \frac{p_{max} - p_{min}}{RT\rho_H} \tag{4}$$

where Δm_{Nm3} represents stored hydrogen volume increase with a pressure change by Δp, p_{max} maximum storage pressure, and p_{min} minimum storage pressure. Thus, it may be assumed that the difference between the minimum and maximum storage pressure is the greatest at the optimum depth.

The maximum pressure is determined at the level of the last casing-shoe depth. The value at which the maximum pressure in the borehole stabilizes is reduced according to the adopted safety factor. Depending on the cavern operation regime and shape, the maximum pressure may also be affected by the potential hydrogen intrusion into the surrounding rocks [45]. In this article, the maximum pressure is defined as:

$$p_{max} = g_f \, h_{cem} \tag{5}$$

The minimum storage pressure depends on the cavern depth, rock salt creeping rate, strength, and cavern size. For the estimation of the salt caverns capacity presented in this article, the minimum storage pressure was approximated by a linear formula (6):

$$p_{min} = g_{pmin} \, (h_{cc} - h_0) \tag{6}$$

where g_{pmin} is minimum storage pressure gradient, h_{cc} is cavern center depth and h_0 maximum depth of the cavern center that may be safely emptied. For further considerations, the values of g_{pmin} = 0.00835 MPa/m and h_0 = 750 m are assumed. The linear shape of formula (6) and the values of the coefficients were adopted on the basis of computer simulations of stress distribution around an empty cavern at various depths and using conservative triaxial salt strenght [68]. Since the g_{pmin} is less than g_f, the difference between the maximum and minimum storage pressures increases with depth. The storage

capacity theoretically increases as well. In practice, however, there are some limitations. High pressures require additional compressors and a particular class of pipes and reinforcement of the borehole. For these reasons, the operating pressure not exceeding 24 MPa is most often applied. There are also limitations due to the compressors' work regime that determines the minimum pressure. In the case of the analyzed CGSF Mogilno, the operation pressure ranges from 3.3 MPa to 21.3 MPa [68].

Based on the above assumptions, calculations of the storage capacity expressed as the amount of hydrogen Δm in [Nm^3] stored in 1 m^3 of cavern volume, were carried out. The calculations consider two variants of storage pressure: I – the only limitation is allowable maximum pressure gradient of 0.016 MPa/m, II – 3.3 MPa to 21.3 MPa corresponding to the CGSF Mogilno. Fig. 4 shows the calculation results. Variant I is marked in blue, and variant II in orange. The maximum depth of the cavern was assumed at a depth of 1800 m bgl.

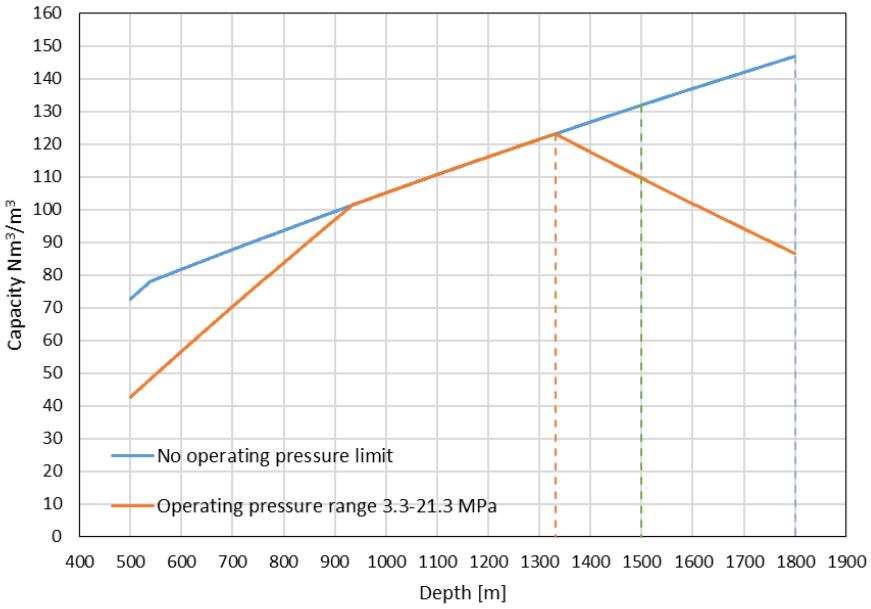

Fig. 4 – Depth-dependent storage capacity after the first injection.

The calculation results show that after the first filling of the salt cavern, the maximum storage capacity for variant I, reached at a depth of 1800 m bgl, is 146.9 Nm^3/m^3. In the case of variant II, the corresponding values are 1331 m bgl and 123.2 Nm^3/m^3, respectively.

3.3. Effect of convergence

Convergence is a phenomenon that leads to salt cavern shrinkage due to salt creep. It is related to the difference between the pressure of the stored hydrogen and the primary pressure of the rock mass,

which is always higher. In addition to the pressure difference, the rate of convergence is significantly affected by temperature, the rheological properties of the rock salt, and the influence of neighboring caverns. The formula (7) defines convergence [68,71]:

$$k(p) = \frac{1}{V}\frac{\partial V}{\partial t} = A_1 \left(\frac{p_\infty(h_{cc}) - p}{\sigma_0}\right)^n e^{-\frac{Q_1}{RT_m}} \tag{7}$$

where *V* represents geometric cavern volume, A_1, n, Q_1 are constant coefficients, *p* cavern pressure, and p_∞ primary lithostatic pressure, defined as follows:

$$p_\infty(h_{cc}) = \left(\rho_o h_{top} + \rho_s\left(h_{cc} - h_{top}\right)\right) g \tag{8}$$

here ρ_o, ρ_s represent the density of overburden rocks and rock salt, h_{top} the salt mirror depth, and T_m rock salt temperature expressed by the formula (9):

$$T_m(h_{cc}) = T_{m0} + g_T\, h_{cc} \tag{9}$$

where Tm_0 is rock mass temperature on the surface (285 K) and g_T geothermal gradient (0.03 K/m).

Assuming two values of coefficient A_1 in the formula (7) in the calculations, two variants of convergence were considered: optimistic ($A_1 = 0.3423‰/year$) and pessimistic ($A_1 = 0.6846‰/year$). Based on the experiments and calculations conducted by [68], the values of the remaining coefficients in formula (7) were defined as follows: $Q_1/R = 2867.9\ K$, $n = 4.089$. In calculations of hydrogen storage capacity of the salt cavern, the following operation scenario was assumed:

1) cavern under the minimum pressure – Δt_{min} = 105 days,
2) cavern filling to the maximum pressure – Δt_{in} = 30 days,
3) cavern under the maximum pressure – Δt_{max} = 200 days,
4) cavern emptying to the minimum pressure – Δt_{exp} = 30 days.

Then the average annual rate of convergence is expressed by the formula (10):

$$\bar{k} = \frac{k(p_{min})\,\Delta t_{min} + k(p_{max})\,\Delta t_{max}}{365} + \frac{k(p_{min})\,(p_\infty - p_{min}) - k(p_{max})\,(p_\infty - p_{max})}{(n+1)\,(p_{max} - p_{min})}\,\frac{\Delta t_{in} + \Delta t_{exp}}{365} \tag{10}$$

The convergence effect was presented on the example of the changes of 1 cubic meter of cavern volume over time. Because of the convergence, after a specific operation time *t,* the volume of one cubic meter of the cavern void will be $\left(1 - \bar{k}\right)^t$ and its storage capacity defines the formula (11):

$$\frac{\Delta m_{Nm^3}}{1m^3} = \frac{p_{max} - p_{min}}{RT\rho_H}\left(1 - \bar{k}\right)^t \tag{11}$$

The results of the calculations indicate that in the case of optimistic convergence after 15 years at depths where maximum storage capacity is recorded, the loss of storage capacity for variant I is about 21% and for variant II only 7%. After 30 years, these values are 27% and 14%, respectively (Fig 5).

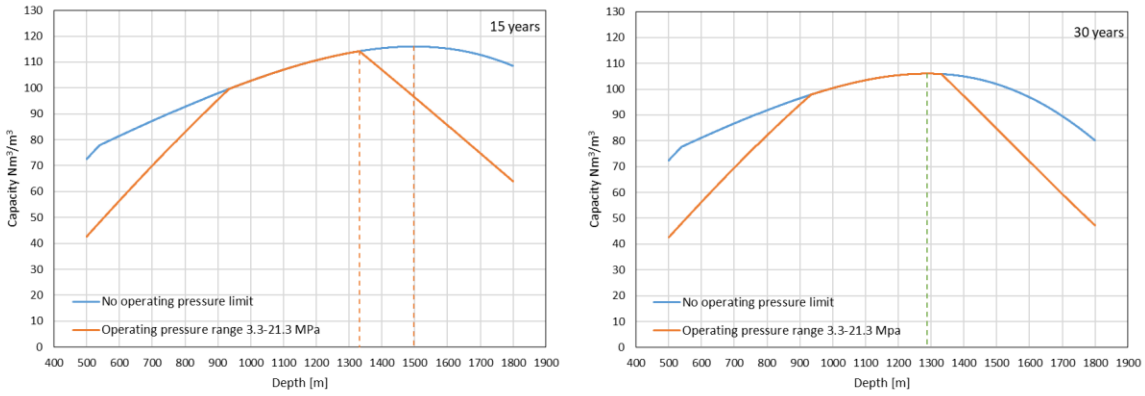

Fig. 5 – Storage capacity depending on depth after 15 and 30 years of cavern exploitation (optimistic convergence variant).

Assuming the pessimistic variant of convergence, we observe much more significant storage capacity loss over time. For example, after 15 years, the loss of storage capacity for variant I is about 27.9%, and for variant II, 14%. After 30 years, these values are 34.2% and 21.5%, respectively (Fig. 6).

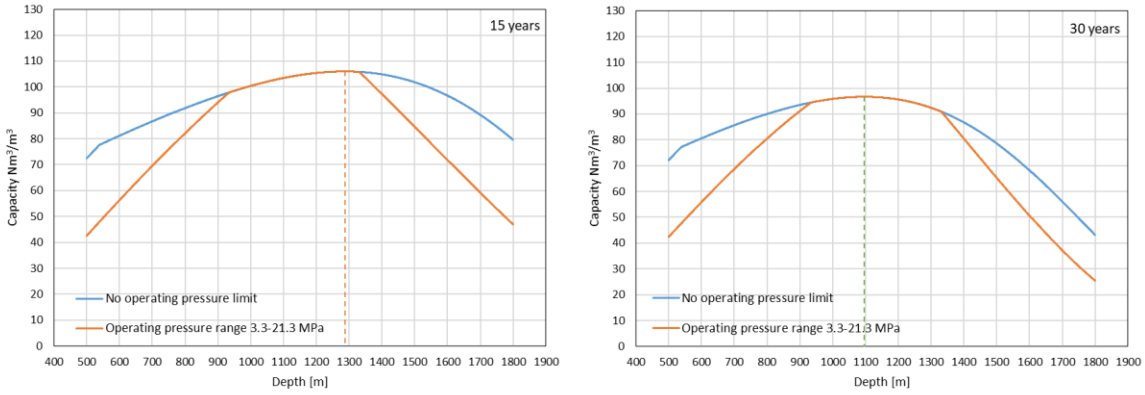

Fig. 6 – Storage capacity depending on depth after 15 and 30 years of cavern exploitation (pessimistic convergence variant).

Figures 7 and 8 show the effect of convergence on the storage capacity in the optimistic and pessimistic variants of convergence. In addition, the figures show the dynamics of changes in the maximum storage capacity and the optimum storage depth depending on the adopted variant of the operating pressure and convergence.

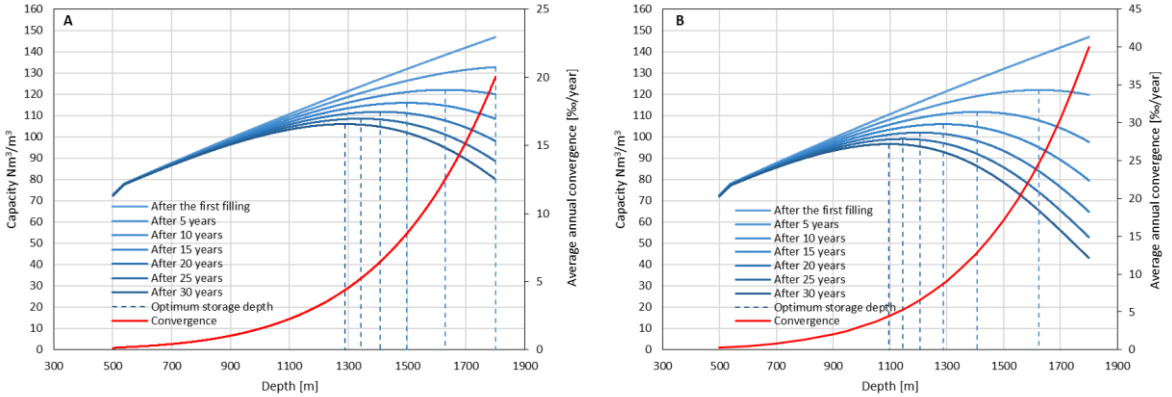

Fig. 7 – Impact of convergence on storage capacity for variant I of storage pressure conditions (A - optimistic, B - pessimistic convergence variant).

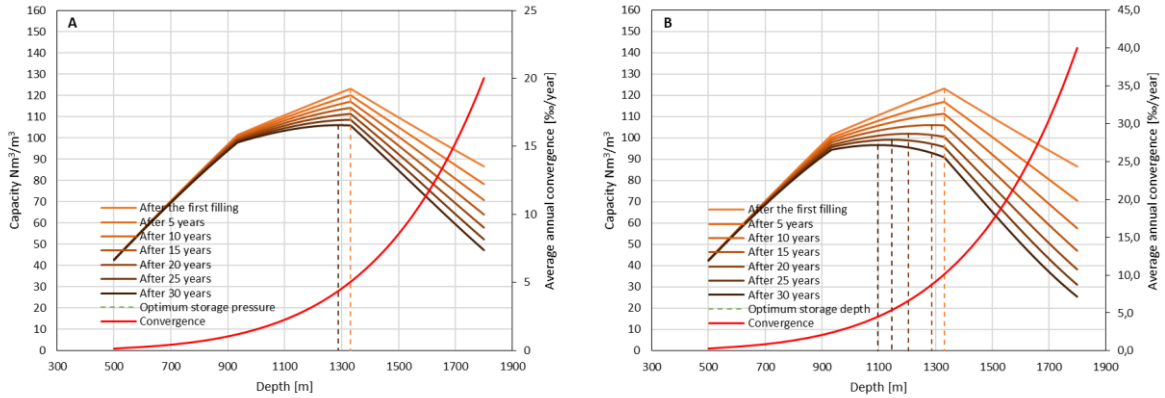

Fig. 8 – Impact of convergence on storage capacity for variant III of storage pressure conditions (A - optimistic, B - pessimistic convergence variant).

Fig. 9 shows, in turn, the changes in maximum capacity over time in function of storage pressure and the convergence rate.

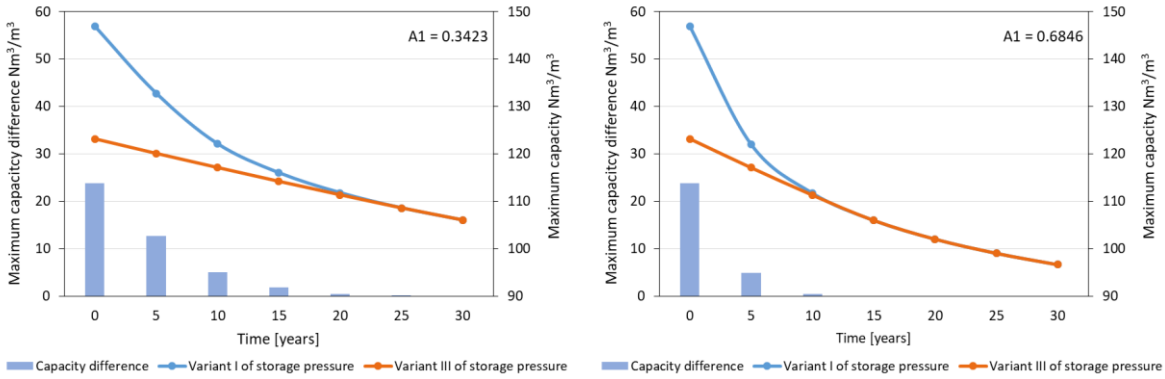

Fig. 9 – Changes in the maximum capacity over time versus the storage pressure range and convergence.

For 30 years corresponding to the average lifetime of the salt cavern, the maximum capacity loss assuming optimistic convergence is 40.9 Nm^3/ m^3 for variant I of storage pressure and 17.2 Nm^3/ m^3 for variant II. These values are correspondingly higher - 50.3 Nm^3/m^3 and 26.5 Nm^3/ m^3, respectively, assuming pessimistic convergence (Fig. 9). The differences in the maximum capacity in the analyzed variants are the greatest in the first years of operation of the caverns. These differences disappear after 20 years for optimistic convergence and after ten years for pessimistic convergence.

Figures 10 -- 12 show surface diagrams of the changes in storage capacity depending on time and depth, taking the operating pressure and convergence variants into account.

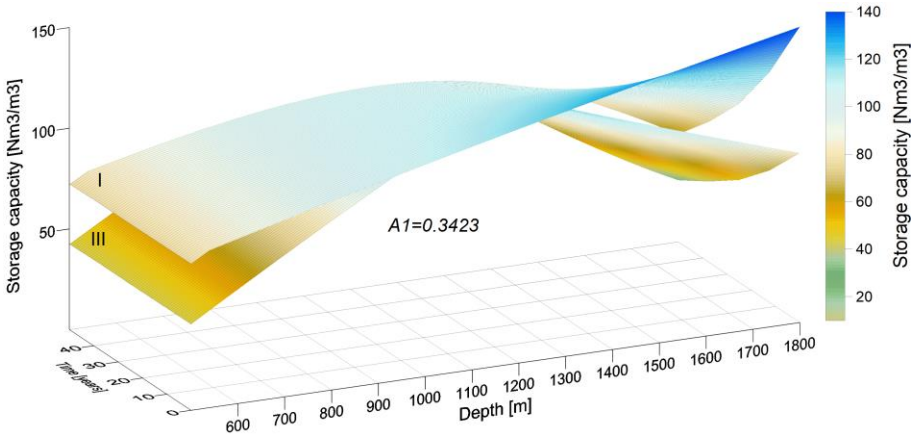

*Fig. 10 – The s*urface plot of the storage capacity for the optimistic variant of the convergence (I, III– variants of storage pressure conditions).

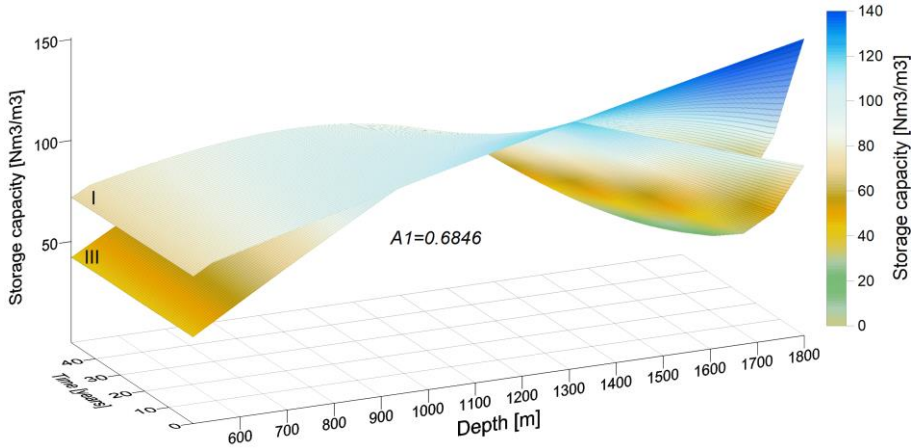

Fig. 11 – The surface plot of the storage capacity for the pessimistic variant of the convergence (I, III– variants of storage pressure conditions).

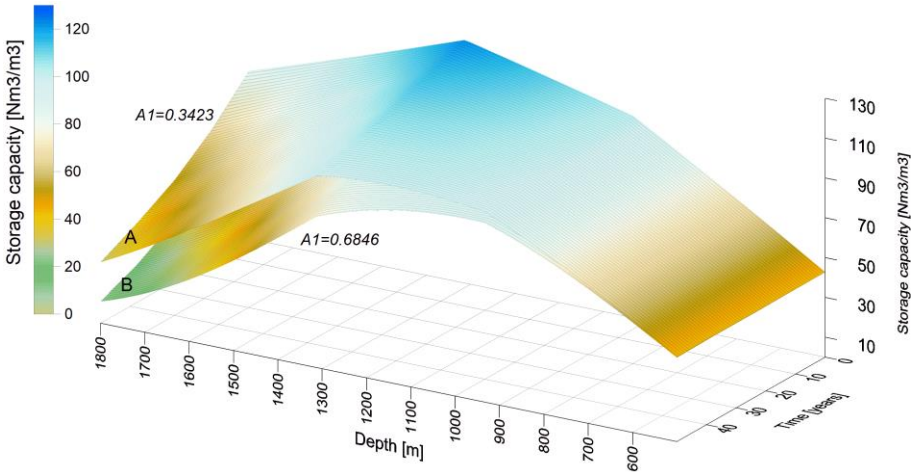

Fig. 12 – The surface plot of the storage capacity - variant I of storage pressure conditions *(A - optimistic convergence variant, B - pessimistic convergence variant).*

The results presented in figures 4 – 12 indicate that the optimum depth of the salt cavern for hydrogen storage is closely dependent on the storage pressure range and convergence rate adopted. Based on the calculations, it may be concluded that the optimum cavern center depth in the case of variant II, the most suitable for the actual storage conditions, is in the range of 1050-1350 m bgl. The optimum depth of 1200 m bgl was assumed for further analysis.

3.4. Statistical analysis of the CGSF Mogilno data

The CGSF Mogilno is the only underground storage facility for compressed gases in the salt dome in Poland. The geological structure, similarly to the remaining Zechstein salt domes in Poland, is very complex. The rock salt layers are steeply dipping, being folded, and faulted. Different solubility of rock salt and accompanying interlayers prevents, in many cases, the construction of a cavern of a designed shape or significantly reduces its volume.

The Mogilno salt dome occurs in central Poland in the NW part of the Mogilno-Łódź Trough. The salt mirror was drilled at 220 to 260 m bgl. Within the salt dome, two separate concessions were issued. In one of them, in the north-western part of the salt dome, the CGSF Mogilno is located (Fig. 13).

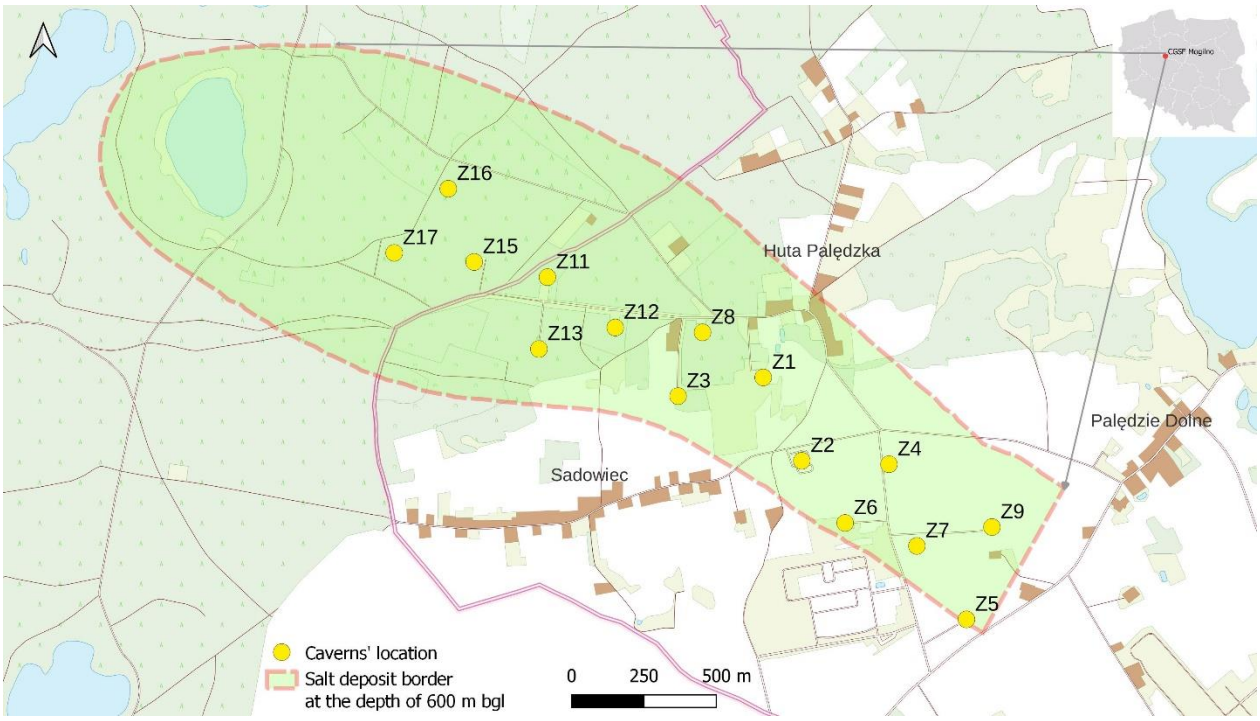

Fig. 13 – The salt cavern location in the CGSF Mogilno [72].

The CGSF Mogilnom includes fifteen caverns. Fourteen of them are currently in operation. In 1995-2005, ten caverns with a total capacity of 416.7 million m^3 were constructed. In the second phase, after 2007, another five caverns were leached. Geological conditions forced the construction of caverns at various depths ranging from 600 to 1600 m bgl. The caverns' shapes are primarily irregular [72], and their working volume ranges from 182000 m^3 to 562000 m^3. The CGSF design assumed the location of the caverns at a distance of about 300 m.

To determine the storage capacity in the Polish salt domes occurring in the same province of the Polish Zechsteinin Basin, the statistical analysis of the storage caverns' depth and volume distributions in the only Polish UGS facility located in a salt dome was performed. Due to the general similarity of the geological structure of the salt domes, the statistical parameters of these distributions were extrapolated to the remaining salt domes, considering the individual A/P coefficients. Statistical analysis made it possible to determine the average depth and volume of caverns (expected values μ) and the probable depth and volume range of caverns in the individual salt domes (standard deviation σ).

3.4.1. Probability of the salt cavern location at a given depth

Based on 15 NG storage caverns in the Mogilno salt dome, the probability of a hydrogen storage cavern location at a given depth was determined. Due to the geological structure, the caverns in the

Mogilno salt dome were located at various depths. Fig. 14. shows the heights and depths of the caverns in the CGSF Mogilno.

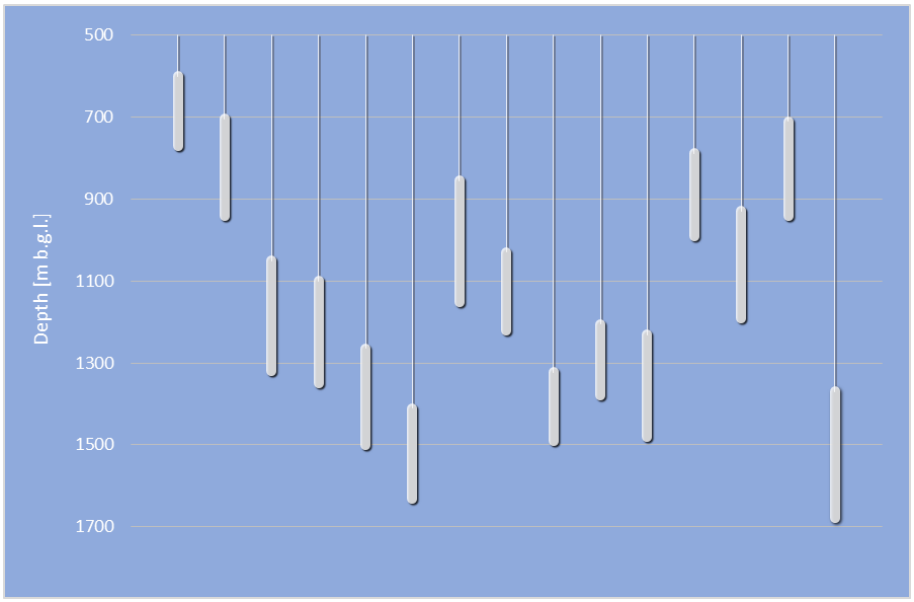

Fig. 14 – The heights and depths of the CGSF Mogilno caverns.

For each cavern of the CGSF Mogilno, a function defining its depth was applied to determine the probability of the cavern location at a given depth. The function is defined by the formula (12):

$$s(h) = \vartheta(h - h_{ct}) - \vartheta(h - h_{cb}) \tag{12}$$

where: ϑ - unit step function (13):

$$\vartheta(x) = \begin{cases} 0 & for\ x < 0 \\ 1/2 & for\ x = 0 \\ 1 & for\ x > 0 \end{cases} \tag{13}$$

The sum of the above functions for 15 caverns determines the number of caverns at a given depth. In order to obtain the histogram describing the probability of a cavern location at a given depth of the Mogilno salt dome, the distribution of the number of caverns depending on depth was normalized to unity.

Fig.15 shows the distribution of the caverns number depending on the depth and the histogram describing the probability of a cavern location at a given depth in the Mogilno salt dome.

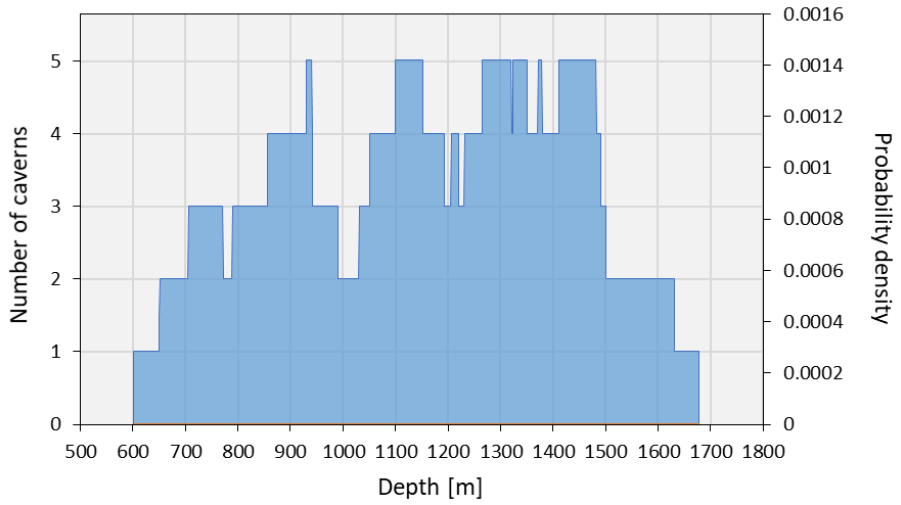

Fig. 15 – Number of the CGSF Mogilno caverns at a given depth (left axis) and probability density of caverns location at a given depth (right axis).

Three theoretical distributions were fitted to the histogram: logistic, trapezoidal, and normal. Fig. 16 shows the fitted probability density functions of the theoretical distributions against the empirical probability of a cavern location at a given depth. The fit quality is represented by individual cumulative distribution functions in Fig. 17. Because of the best fit, for further considerations, the trapezoidal distribution was adopted.

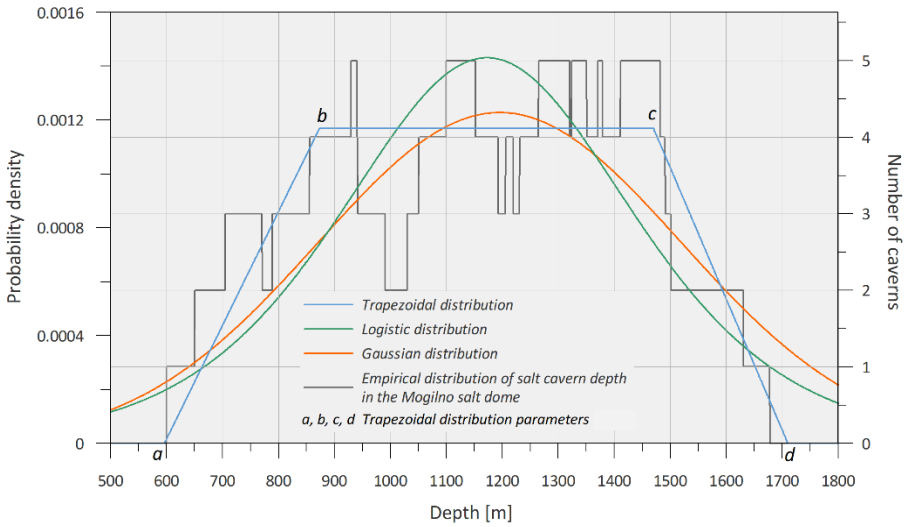

Fig. 16 – Probability density of theoretical distributions of salt caverns location at a given depth based on the CGSF Mogilno data.

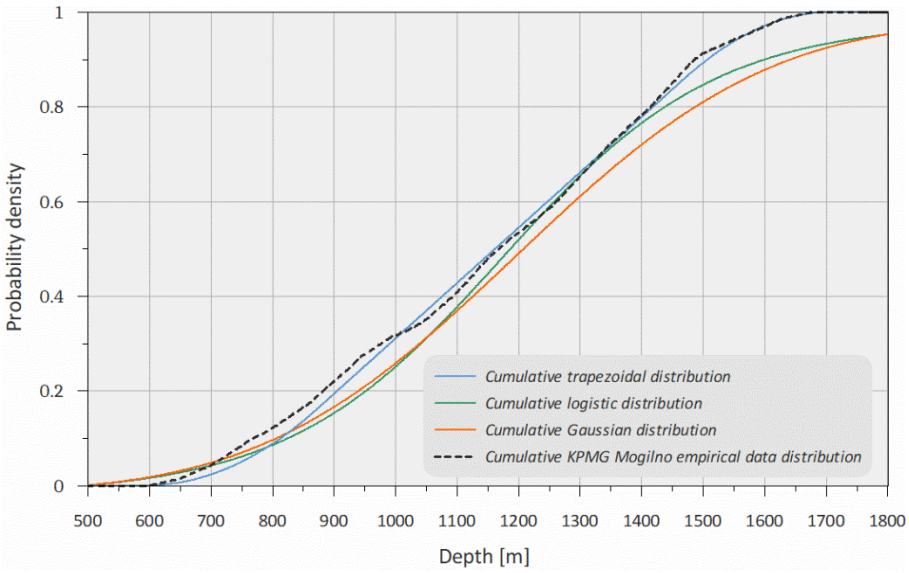

Fig. 17 – Empirical and theoretical cumulative distribution functions of salt caverns location at a given depth based on the CGSF Mogilno data.

Because of the best fit for further considerations, the trapezoidal distribution was adopted. The probability density of the trapezoidal distribution was calculated by the formula (14):

$$f(h) = \begin{cases} \frac{2}{(b-a)\,(d+c-b-a)}\,h - \frac{2a}{(b-a)\,(d+c-b-a)} & for\ a \le h < b \\ \frac{2}{(d+c-b-a)} & for\ b \le h < c \\ \frac{-2}{(d-c)\,(d+c-b-a)}\,h + \frac{2d}{(d-c)\,(d+c-b-a)} & for\ c \le h \le d \end{cases} \quad (14)$$

The expected value of the trapezoidal distribution, reflecting the average cavern depth, is determined by the formula (15):

$$\mu = \frac{d^2+c^2+cd-b^2-a^2-ab}{3\,(d+c-d-a)} \quad (15)$$

and the variance by the formula (16):

$$\sigma^2 = \frac{d^2+d^2c+cd^2+c^3-b^3-b^2a-ab^2-a^3}{6\,(d+c-d-a)} - \mu^2 \quad (16)$$

For the trapezoid distribution the expected value and standard deviation are: μ = 1161,32 m, σ = 258,043 m. The adjusted distribution parameters are as follows: a = 596 m, b = 873 m, c = 1470 m, d = 1710 m.

3.4.2. Probability of the salt cavern construction of a given volume

The second analyzed parameter was the volume of salt caverns. The volume of salt caverns in the Mogilno salt dome structure ranges from 182 000 m^3 to 562 000 m^3. The volume histogram, representing the distribution of the caverns' volume in the Mogilno salt dome, was obtained by introducing a moving volume range of 100 000 m^3 due to the small amount of the empirical data (number of caverns). The range was checked every 20 000 m^3 in terms of the number of caverns, the volume of which was within the analyzed range. Twenty-four ranges from 100 000 m^3 to 600 000 m^3 were analyzed. The range positions are not statistical classes because they are not disjoint. The applied procedure is equivalent to the disjoint classes with a width of 20 000 m^3 with a 5-point smoothing filter.

Fig. 18 shows the histogram describing the probability of a cavern construction of a given volume in the Mogilno salt dome and the fitted probability density functions of the theoretical distributions. The quality of the fit is represented by the individual cumulative distribution functions in Fig. 19.

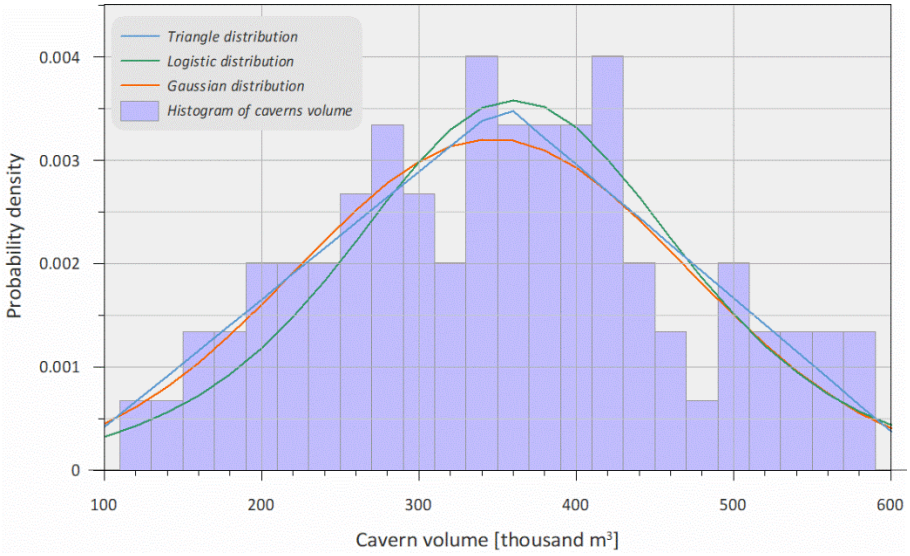

Fig. 18 – Probability density of a cavern construction of a given volume based on the CGSF Mogilno data and fitted theoretical distribution.

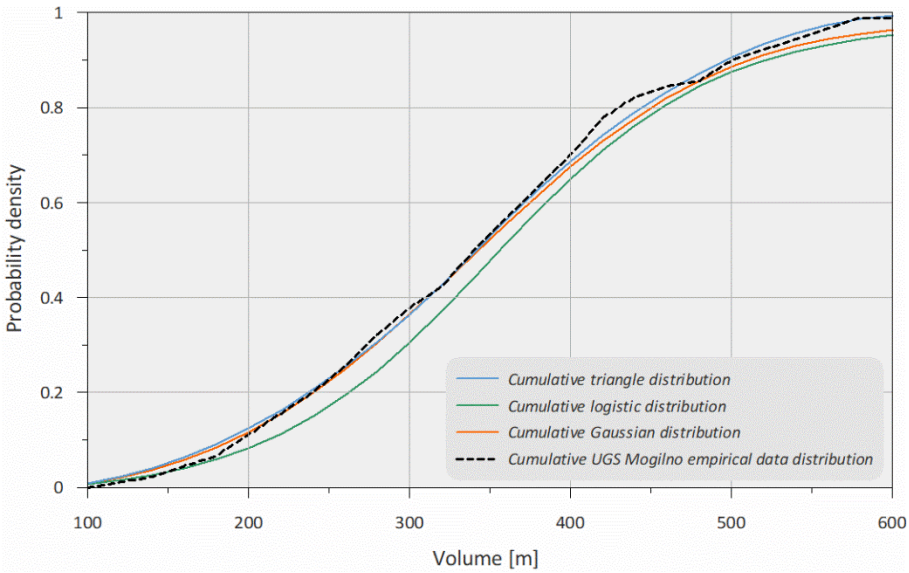

Fig. 19 – Empirical and theoretical cumulative distribution functions of a given volume cavern construction probability based on the CGSF Mogilno data.

The triangular distribution, defined by the formula (17), was chosen for further consideration due to the best fit.

$$f(V) = \begin{cases} \frac{2(V-V_1)}{(V_2-V_1)\,(V_0-V_1)} & for\ V_1 \le V \le V_0 \\ \frac{2(V_2-V)}{(V_2-V_1)\,(V_2-V_0)} & for\ V_0 \le V \le V_2 \end{cases} \tag{17}$$

The expected value in a triangular distribution is given by the formula (18):

$$\mu = \frac{V_1+V_2+V_3}{3} \tag{18}$$

and the variance by the formula (19):

$$\sigma^2 = \frac{V_1^2+V_0^2+V_2^2-V_1V_0-V_2V_0-V_1V_2}{18} \tag{19}$$

The parameters of the triangular distribution are: V_1 = 66 000m^3, V_0 = 354 000 m^3, V_2 = 629 000 m^3. The expected value representing the average cavern volume is 349 700 m^3, and the standard deviation is 114 900 m^3.

3.4.3. Statistical parameters of the selected salt domes

The generalization of the statistical parameters of probability distributions of the cavern depth and volume determined for the CGSF Mogilno to other salt domes requires considering the differences in the quantitative share of rock salt layers suitable for cavern construction and in the depth of the salt

mirror in the individual salt domes. Therefore, to assess the share of rock salt layers suitable for cavern construction, an analysis of the geological structure of selected salt domes at the surface of the salt mirror was carried out. Since anticlinal structures, including rock salt, are privileged for cavern construction, the analysis has been carried out by Ślizowski [73] to determine the ratio of the anticlinal structures surface area (A), at a depth of the salt mirror, to the surface area of the analyzed salt dome (P) at the same depth. The results of the analysis and archival data review [73] are shown in Table 2.

Table 2. The surface area of the selected salt domes (P) and anticlinal structures (A) at the salt mirror depth and the (A/P) coefficients based on [73]

Salt dome	P [km^2]	A [km^2]	A/P
Damasławek	16.5	6.06	0.367
Dębina	0.5	0.44	0.880
Góra	1.0	0.74	0.740
Inowrocław	2.0	1.28	0.640
Izbica Kujawska	4.0	2.24	0.560
Kłodawa	37.5	12.3	0.328
Lubień	5.9	3.0	0.508
Łanięta	9.5	4.37	0.460
Mogilno	7.5	3.3	0.440
Rogóźno	21.0	7.89	0.376
Wapno	0.3	0.267	0.890

Fig. 20 shows the relationship between the normalized share of anticlinal structures and the surface area of the selected salt domes at the salt mirror depth and the A/P power function fit.

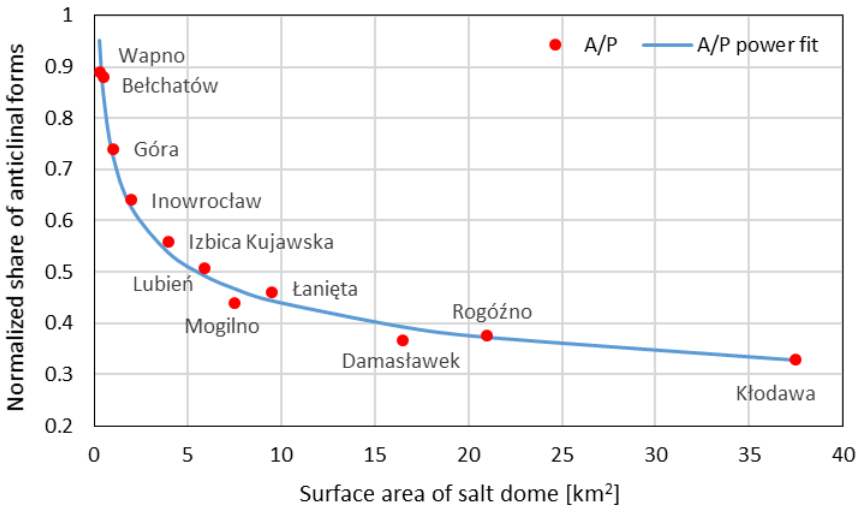

Fig. 20 – The normalized share of anticlinal structures against the salt dome surface area at the salt mirror depth and the A/P function fit.

It may be concluded that the smaller the A/P coefficient, the more difficult it is to construct the cavern in the selected salt dome, considering the relationship presented in Fig. 20. Therefore it was assumed that the relations between the cavern depth distribution parameters correspond to the relationship between the respective A/P coefficients of the selected salt domes. Then, the expected value of the depth distribution in the considered salt dome μ may be defined as follows:

$$\mu = \mu_M \frac{(A/P)_M}{(A/P)} \tag{20}$$

where μ_M represents the expected value of a cavern volume in the Mogilno salt dome, *(A/P)* value of the coefficient for the selected salt dome, and $(A/P)_M$ = 0,44 value of the coefficient for the Mogilno salt dome. The standard deviation of the depth distribution in the considered salt dome (σ) is:

$$\sigma = \sigma_M \frac{(A/P)_M}{(A/P)} \tag{21}$$

The value of parameter *a* was defined as:

$$a = a_M \frac{(A/P)_M}{(A/P)} \tag{22}$$

The remaining distributions parameters *b, c, d,* and V_0, V_1, V_2 were defined in the same way.

If the value of the parameter *a* of the trapezoidal distribution, specifying the minimum depth of a cavern, was lower than the depth of the salt mirror increased by 100 m (the thickness of the rock salt above a cavern), then it was decreased so that its value was equal to the salt mirror depth + 100 m. When the expected value μ, determining the average depth of cavern, was lower than the optimum depth of the cavern center, i.e., 1200 m, then its value was adjusted to the optimum depth to improve cavern storage capacity.

Similarly, to obtain the value of the average cavern size in the selected salt domes, the statistical parameters of the cavern volume distribution for the Mogilno salt dome were generalized to other salt domes, assuming proportionality between the A/P coefficient of the selected salt domes. Table 3 presents the estimation results of the caverns' volume and depth for individual salt domes.

Table 3. Statistical parameters of storage caverns in the selected salt domes.

Salt dome	*A/P*	Average cavern volume [thousand m^3]	The standard deviation of average volume [thousand m^3]	Average depth [m bgl]	The standard deviation of average depth [thousand m^3]
Damasławek	0.367	295.5	137.7	1409	324.7
Dębina	0.837	673.5	60.4	1200	151.3
Izbica Kujawska	0.560	450.5	99.5	1200	221.8
Kłodawa	0.328	263.9	90.3	1705	444.1
Lubień	0.508	409.1	154.2	1200	242.9
Łanięta	0.460	370.1	109.9	1200	275.0
Mogilno	0.440	354.0	114.9	1161	258.0
Rogóźno	0.376	302.3	134.6	1345	352.5

Fig. 21 and 22 show the average values and standard deviation of caverns depth and volume in the selected salt domes.

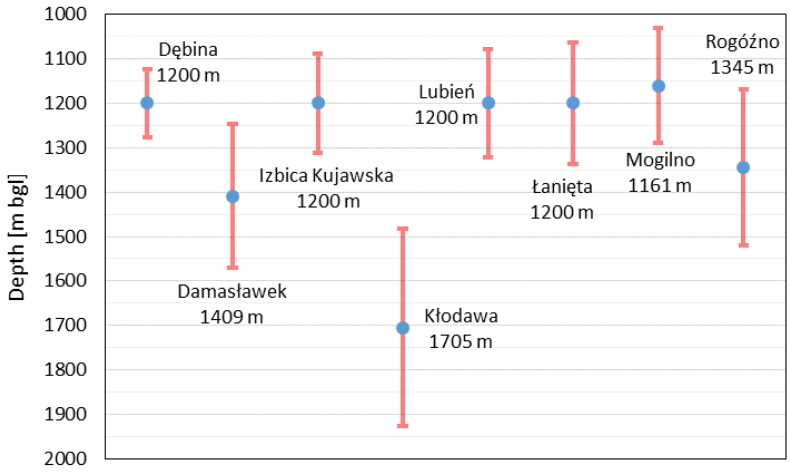

Fig. 21 – The average values and the standard deviation of the depth of the caverns in the selected salt domes.

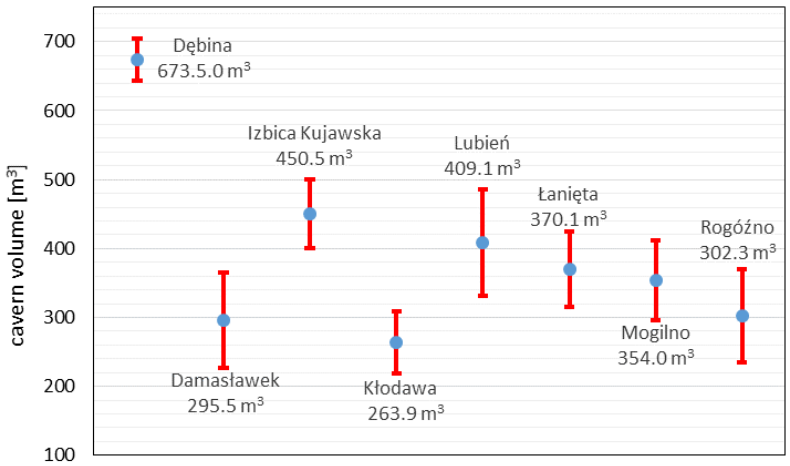

Fig. 22 –The average values and the standard deviation of the volume of the caverns in the selected salt domes.

The analysis carried out indicates that in the case of four salt domes (Dębina, Izbica Kujawska, Lubień, and Łanięta), it is possible to construct caverns at the optimum depth, i.e., 1200 m bgl. Because of the small share of anticlinal structures at the salt mirror depth and the relatively large area, the average depth of caverns in the Kłodawa salt dome is 1704 m bgl. The average values of the cavern volume in individual salt domes do not differ significantly from each other and fall within the range of 263 900 – 450 000 m^3. However, this value varies considerably in the case of the Dębina salt dome, reaching 673 500 m^3. This difference is mainly due to the high share of anticlines in this salt dome.

4. Calculation of the storage potential of salt domes

The calculations assume the caverns' triangular grid layout and the distance between caverns axes of 250 m. With such a caverns layout, the surface area assigned to a single cavern is:

$$S = 250^2 \frac{\sqrt{3}}{2} = 54126.6\ m^2 \tag{23}$$

The amount of hydrogen stored in a single cavern is determined according to the formula (24):

$$m_{Nm^3} = \frac{pV}{\rho_H RTZ} \tag{24}$$

When calculating the average storage potential, a linear temperature rise with depth, a pessimistic variant of convergence, the value of the average annual convergence based on formula (10), and the use of 80% of the cavern geometric volume were assumed. The storage potential per 1 km^2 of the salt dome area, taking convergence into account, is expressed by the formula (25):

$$C = \frac{fV\Delta_p}{S\rho_H RTZ}\left(1-\bar{k}\right)^l \quad (25)$$

where *f* represents the ratio of the hydrogen-filled cavern volume to its total volume (0.8).

Table 4 presents the results of the calculations, based on the values obtained from the statistical analysis, showing the average storage capacity of caverns in M Nm^3, the average storage capacity of the salt domes in billion Nm^3, and the average storage capacity per area expressed in billion Nm^3/km^2.

Table 4. Results of the average storage capacity calculations for the selected salt domes

Salt dome	Salt dome surface area [km^2]	Number of caverns	Average cavern volume [thousand m^3]	Average cavern depth [m bgl]	Average cavern capacity after first filling [M Nm^3]	The average capacity of the salt dome [B Nm^3] over time [years]			The average capacity of the salt dome [B Nm^3/km^2] over time [years]		
						0	15	30	0	15	30
Damasławek	16.5	304	295.5	1409	27.6	8.40	6.91	5.68	0.51	0.42	0.34
Dębina	0.5	9	673.5	1200	65.5	0.59	0.51	0.45	1.21	1.05	0.92
Kłodawa	21.0	387	263.9	1705	19.8	7.66	4.78	2.98	0.37	0.23	0.14
Izbica Kujawska	4.0	73	450.5	1200	43.8	3.20	2.79	2.43	0.81	0.71	0.62
Lubień	5.9	109	409.1	1200	39.8	4.34	3.78	3.30	0.73	0.64	0.56
Łanięta	9.5	175	370.1	1200	36.0	6.30	5.49	4.79	0.66	0.58	0.51
Mogilno	7.5	138	354.0	1161	32.3	4.46	4.09	3.76	0.60	0.55	0.50
Rogóźno	21.0	387	302.3	1345	29.5	11.42	9.75	8.31	0.55	0.47	0.40

For further analysis, the storage capacity of the selected salt domes expressed in Nm^3 was converted to the thermal energy of the stored hydrogen represented in TWh_t, assuming the hydrogen calorific value of 10.8 MJ/m^3. Fig. 23 shows changes in the average storage capacity of the salt domes in the thermal energy of stored hydrogen over 30 years.

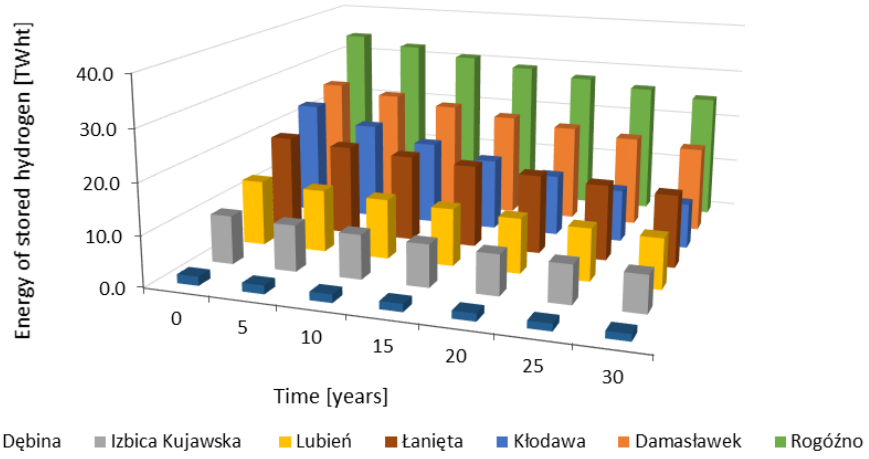

Fig. 23 – The average thermal energy of the stored hydrogen in the selected salt dome.

The most significant storage capacity was noted in the case of the Rogóźno salt dome – from 34.3 TWh_t after the first filling to 24.9 TWh_t after 30 years. Such a storage capacity is due to the salt dome's size and the caverns' depth, ensuring moderate cavern convergence. On the other hand, in the case of the Kłodawa salt dome, despite a similar surface area, we observe a much lower storage capacity – from 23.0 TWh_t to only 10.0 TWh_t, respectively. The reason is the 350 m deeper location of salt caverns, causing the convergence rate to increase. To present the storage potential, the authors assumed that all caverns in the selected salt domes started operating simultaneously. The assumption is, of course, hypothetical and is applied to compare the storage capacity between the individual salt domes. Fig. 24 shows the calculation results of the average storage potential of the selected salt domes over 30 years.

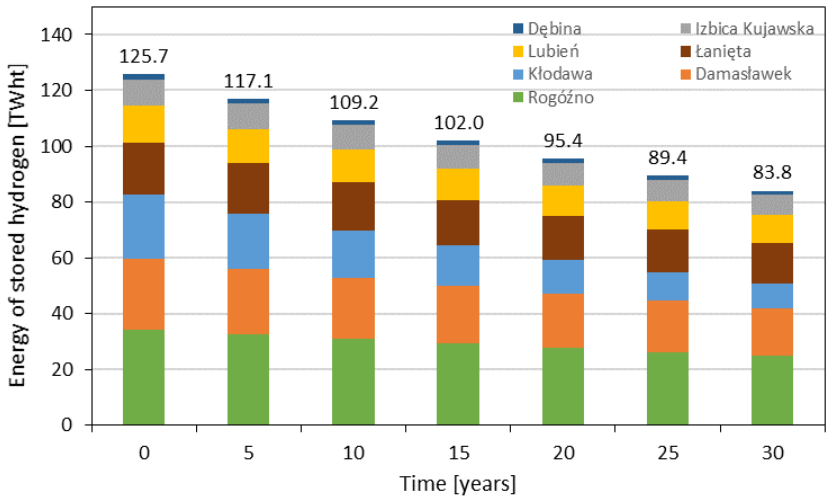

Fig. 24 – The total average storage potential of the selected salt domes over the operation period.

According to estimates, the total storage potential in individual years ranges from 125. 7 TWh_t after the first filling to 83.8 TWh_t after 30 years of operation. The total average storage potential of the individual salt domes over 30 years was determined, considering the operation scenario covers one cycle of filling and emptying per year. Fig. 25 shows the result of the calculations.

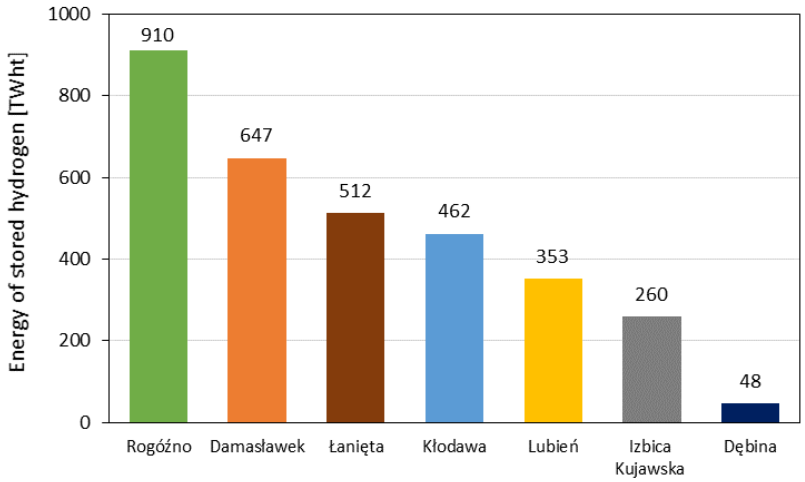

Fig. 25 – The average storage capacity of individual salt domes, assuming one storage cycle annually for 30 years of operation.

According to the estimates, the highest hydrogen average storage potential of 910 TWh_t was noted for the Rogóźno salt dome. In contrast, all salt domes' hydrogen average storage potential reaches 3193 TWh_t after 30 years.

Salt caverns construction at the optimum depth, the maximum cavern volumes resulting from the statistical analysis, and the optimistic variant of convergence were assumed to assess the maximum hydrogen storage potential of the selected salt domes. The optimum depth of the cavern center was considered as 1300 m bgl. Since the methodology does not assume the same depth of caverns in the salt dome, the maximum storage capacity of the selected salt domes depending on the cavern depth was presented in Fig. 26, considering the expected caverns' volume.

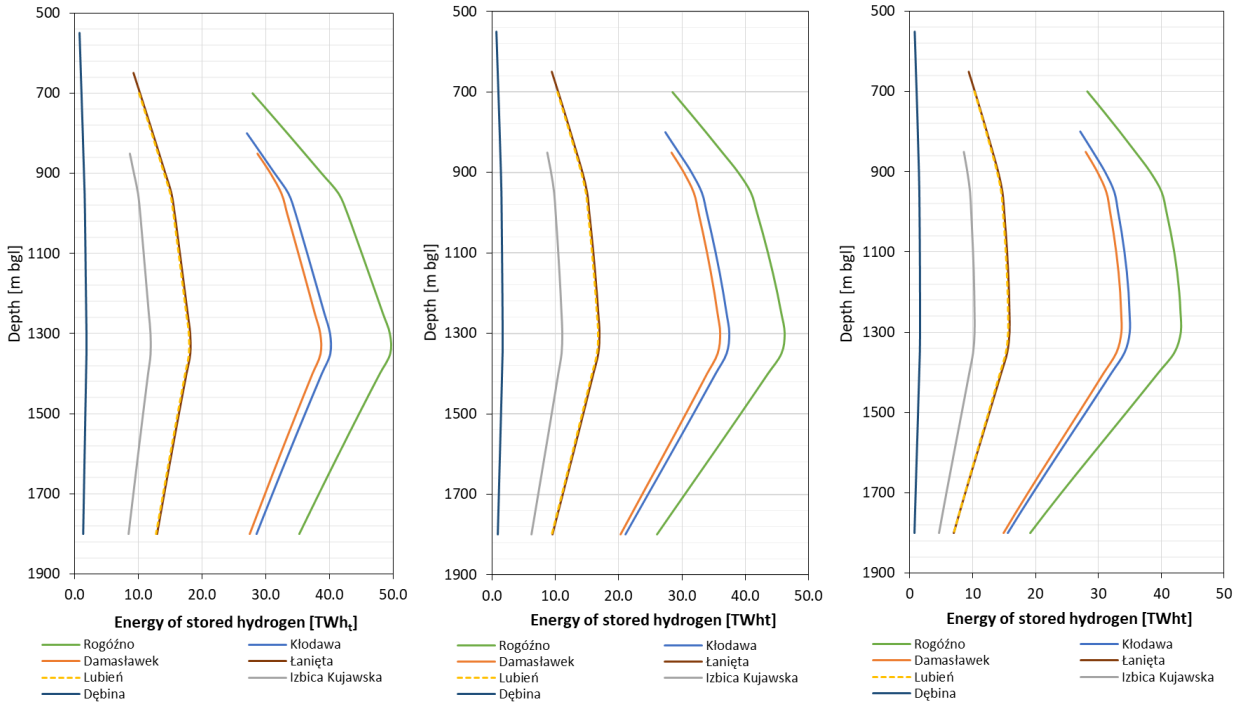

Fig. 26 – The maximum hydrogen storage capacity of salt domes against the cavern center depth.

Fig. 27 shows the comparison of the maximum and average hydrogen storage potential assessed based on the presented methodology considering the maximum and expected caverns' volume.

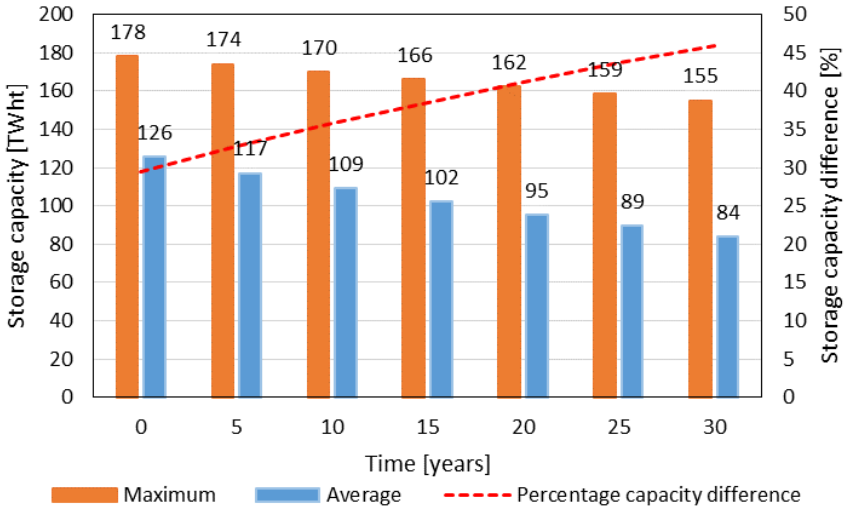

Fig. 27 – The comparison of the maximum and average hydrogen storage potential of the selected salt domes over the operation period.

The analysis showed that after first filling, the maximum hydrogen storage potential of the selected salt domes exceeds the average storage capacity of about 30%. This difference increases with the time of caverns operation and reaches 47% after 30 years.

5. Discussion

In the methodology for assessing the hydrogen storage potential in salt domes, particular attention was paid to the most relevant factors in this regard: cavern size, depth, and the impact of convergence on the capacity of the storage cavern. A similar approach can be found in numerous publications, including [21,51,74].

The assessment of the maximum height of the salt cavern is an essential factor due to its stability and the risk of fracturing the salt formation when emptying the cavern. Therefore, based on the maximum allowable pressure gradient of 0.016 MPa/m [52], the authors analyzed the maximum possible height of caverns. The estimates show that with conservative assumptions, at a depth of 1000 m bgl, it is possible to construct caverns with a maximum height of 300 m, providing a large storage capacity. However, there is a low probability of leaching caverns with the maximum depth resulting from these estimates, considering the geological structure of Polish salt domes.

The salt cavern convergence is a significant factor in assessing their capacity. The convergence rate is significantly affected by temperature, the rheological properties of the rock salt, the influence of neighboring caverns, operational scenario, and cavern shape and size [58,75,76]. The estimates of salt cavern convergence include two values of the coefficient (A_1) determined based on previously conducted research [68]. Similarly, as in other analyses, a seasonal hydrogen storage operation scenario to balance energy demand was assumed [5,40,41]. In the case of storage pressure range of 3.3 – 21.3 MPa, considering the optimistic convergence variant, 15 years after the first filling of the cavern with hydrogen, a decrease in storage capacity of 7% is observed. After 30 years, this value reaches 13.9%. In the case of the pessimistic convergence variant, the values are 14.0% and 21.5%, respectively. Similar decreases in storage capacity were observed for NG caverns [77]. The presented values correspond to the results of calculations presented by [78–81].

The capacity of caverns was found to vary throughout the operation cycle. It was observed that over the 30-year operation cycle of the salt cavern, the loss of the storage capacity might reach even 26.5 Nm^3/m^3 assuming the pessimistic variant of convergence. The differences in the maximum capacity in the analyzed variants of the operating pressure ranges and convergence are the largest in the initial

years of operation. In the case of the optimistic convergence variant, these differences disappear after 20 years, for the pessimistic variant - after ten years. Calculations indicate that the optimum depth of a salt cavern for hydrogen storage is closely dependent on the operating pressure range and convergence rate adopted. In the pressure range considered corresponding to actual storage conditions, the optimum cavern center depth is in the range of approximately 1050 to 1350 m bgl, similar to the NG storage caverns [68].

Thus, the statistical analysis was applied to determine the expected storage cavern depth and volume values in the selected salt domes, considering their geological structure. The authors are not aware of similar studies on the influence of the geological structure on the storage capacity of salt domes.

The estimates of the storage capacity of salt caverns in Europe presented so far [34] are based on arbitrary assumptions about the size of salt caverns. Such assumptions lead to significant simplifications and inaccuracies related to the scale of the estimates made. The presented estimates, taking into account the essential factors influencing the storage capacity of salt domes, such as the caverns size, their optimum depth, and convergence as well as the geological structure of individual salt domes, are the next stage of detailed evaluation of the hydrogen storage potential of salt domes. Therefore, the obtained results, based on the application of the original method, allowed us to significantly refine the estimates of the storage capacity of the salt domes, compared to those presented by Caglayan et al. [34], which estimate the storage potential of bedded formations and salt domes in Poland at approx. 10000 TWh_t. Estimates of the storage potential of rock salt deposits occurring in the southern part of the Zechstein salt basin in Poland [44] indicate that their maximum capacity does not exceed 1000 TWh_t. Due to their size, the total storage potential of salt deposits in Poland should be much lower than in the previous forecasts [34].

It should be noted that the presented values of the hydrogen storage potential of salt domes correspond to the technical storage potential considering only geological and mining conditions. Therefore, one should expect that the actual storage potential of the salt domes will be much lower when taking into account all surface and underground barriers that constrain the salt cavern's construction, as indicated by Juez-Larré et al. [37] and Tarkowski and Uliasz-Misiak [82].

The estimates indicate that the Rogóźno salt dome has the highest storage potential, from 34.3 TWh_t after the first filling to 24.9 TWh_t after 30 years. This storage potential loss is due to the size and depth of the cavern, ensuring its moderate convergence. Considering the assumed operating scenario, the average storage capacity of the selected salt domes ranges from 125.7 TWh_t after first filling to 83.8 TWh_t after 30 years of operation. The average loss in storage capacity of the selected salt domes was estimated

at 33% of the initial capacity. This value varies significantly between salt domes. The capacity losses that result from convergence range from 23.3% in the case of salt caverns located at a depth of 1200 m bgl to 61% in the case of caverns located at a depth of about 1700 m bgl (the Kłodawa salt dome). As indicated in previous publications, the cavern convergence depends on depth, rheological properties of the rock salt [83–85], and thermo-mechanical conditions [21,75,76].

The estimates show that assuming the seasonal operating scenario, the energy of the stored hydrogen in the Rogóźno salt dome might reach even 910 TWh_t over 30 years of operation. The analysis of the maximum storage capacity considering the optimum caverns' depth, maximum caverns' volume, and optimistic convergence indicates that the selected salt domes' total storage capacity ranges from 178 TWh_t after the first filling to approx. 156 TWh_t after 30 years of operation. The analysis of changes in the storage capacity of the salt domes over time indicates that their maximum total storage capacity exceeds the average of 29%. This difference increases with the time of cavern exploitation, and in the case of the selected salt dome, it reaches over 45% after 30 years. Changes in the storage capacity are related to the properties of rock salt and thermomechanical conditions during cavern exploitation, which was also noted by [86–88].

The obtained results may inspire the EU countries interested in developing UHS and energy storage in salt domes. Geological survey organizations may also use the methodology to assess hydrogen storage capacity. The methodology application allows the optimal areas for hydrogen storage to be determined and related to areas of energy production from RES. Specific salt domes may interest energy, chemical, or petrochemical companies looking for UHS sites. The methodology presented, with appropriate modifications, may also be used to estimate the storage capacity of other gases.

8. Conclusions

The methodological basis for the detailed assessment of the storage potential of salt domes requires considering the analysis of the size of the hydrogen storage cavern depending on its depth, the optimum depth of the hydrogen storage cavern, and the impact of convergence on the cavern capacity during its operation. When assessing the storage capacity of salt domes, it is essential to consider their complex geological structure, which limits the cavern depth and size. During the storage of hydrogen in salt dome caverns, there is a significant decrease in storage capacity compared to the state after the first filling of the cavern, which increases with the storage period.

Assuming the cavern operation scenario covers one full cycle of filling and withdrawal per year, it can be seen that the energy of the stored hydrogen in the case of large salt domes may reach as much as 910 TWh_t over a 30-year operating period.

Estimates of the storage capacity of salt domes in Poland, based on the proposed methodology, indicate at least an order of magnitude lower storage potential than the previously presented calculations. However, there is still a vast storage potential of approximately 10 Mt of hydrogen, significantly exceeding the national demand for hydrogen use in electricity generation considering the International Energy Agency forecast indicating global demand at about 50 Mt in 2030 [89].

The values presented correspond to the technical storage potential considering only geological and mining conditions; the actual capacity of the salt domes may turn out to be much lower after considering surface and underground conditions using spatial data analysis tools.

Acknowledgments

This work was supported by the Mineral and Energy Economy Research Institute of the Polish Academy of Sciences (research subvention).

The authors (Radosław Tarkowski and Leszek Lankof) participate in EU project Hystories - Hydrogen Storage In European Subsurface. This project has received funding from the Fuel Cells and Hydrogen 2 Joint Undertaking under grant agreement No. 101007176. This Joint Undertaking receives support from the European Union's Horizon 2020 research and innovation program Hydrogen Europe and Hydrogen Europe Research.

Credit author statement

Leszek Lankof: Conceptualization, Methodology, Investigation, Formal analysis, Visualization, Supervision, Writing Original Draft, Review and Editing. Kazimierz Urbańczyk: Conceptualization, Methodology, Investigation, Formal analysis, Validation, Review and Editing. Radosław Tarkowski: Conceptualization, Methodology, Investigation, Writing Original Draft, Review and Editing.

Declaration of competing interest

The authors declare that they have no known competing financial interests or personal relationships that could have appeared to influence the work reported in this paper.

References

[1] Crotogino F, Donadei S, Bünger U, Landinger H. Large-Scale Hydrogen Underground Storage for Securing Future Energy Supplies. In: Stolten D, Grube T, editors. 18th World Hydrogen Energy Conference 2010 - WHEC 2010 Parallel Sessions Book 4: Storage Systems/Policy Perspectives, Initiatives and Co-operations. Essen: Forschungszentrum Jülich GmbH, Zentralbibliothek, Verlag Schriften; 2010. p. 10.

[2] Wolf E. Large-Scale Hydrogen Energy Storage. In: Moseley PT, Garche J, editors. Electrochemical Energy Storage for Renewable Sources and Grid Balancing. Elsevier B.V.; 2015. p. 129–42.

[3] Kruck O, Crotogino F. Benchmarking of Selected Storage Options. Hannover; 2013.

[4] Andersson J, Grönkvist S. Large-scale storage of hydrogen. Int J Hydrogen Energy. 2019;44(23):11901–19.

[5] Evans J, Shaw T. Storage of Hydrogen in Solution Mined Salt Caverns for Long Duration Energy Storage. In: SMRI Spring 2021 Virtual Technical Conference. Solution Mining Research Institute; 2021. p. 1–20.

[6] Caglayan DG, Heinrichs HU, Robinius M, Stolten D. Robust design of a future 100% renewable european energy supply system with hydrogen infrastructure. Int J Hydrogen Energy. 2021;46(57):29376–90.

[7] Abdin Z, Zafaranloo A, Rafiee A, Mérida W, Lipiński W, Khalilpour KR. Hydrogen as an energy vector. Renew Sustain Energy Rev. 2020;120(November 2019).

[8] Gabrielli P, Poluzzi A, Kramer GJ, Spiers C, Mazzotti M, Gazzani M. Seasonal energy storage for zero-emissions multi-energy systems via underground hydrogen storage. Renew Sustain Energy Rev. 2020;121:109629.

[9] Foh S, Novil M, Rockar E, Randolph P. Underground hydrogen storage. Institute of Gas Technology, DOE, Brookhaven National Lab, Upton, NY. New York; 1979.

[10] Panfilov M. Underground and pipeline hydrogen storage. Compendium of Hydrogen Energy. Elsevier Ltd.; 2016. 91–115 p.

[11] Tarkowski R. Underground hydrogen storage: Characteristics and prospects. Renew Sustain Energy Rev. 2019;105:86–94.

[12] Acht A, Donadei S. Hydrogen Storage in Salt Caverns State of the Art, New Developments and R&D Projects. In: SMRI Fall 2012 Technical Conference. Bremen; 2012.

[13] Kruck O, Crotogino F, Prelicz R, Rudolph T. Overview on all Known Underground Storage Technologies for Hydrogen Deliverable No. 3.1 [Internet]. 2013. Available from: http://hyunder.eu/wp-content/uploads/2016/01/D3.1_Overview-of-all-known-underground-storage-technologies.pdf.

[14] Tarkowski R, Czapowski G. Salt domes in Poland – Potential sites for hydrogen storage in caverns. Int J Hydrogen Energy. 2018;43(46):21414–27.

[15] Zander-Schiebenhöfer D, Donadei S, Horvath P-L, Zapf D, Staudtmeister K, Rokahr RB, et al. Basic Data, Information System & Potential Estimation for Site Selection of Salt Caverns for Energy Storage. In: SMRI Fall 2015 Technical Conference. Santander: Solution Mining Research Institute; 2015. p. 1–12.

[16] Horvath P-L, Mirau S, Schneider G, Heike B, Weiler C, Bödeker J, et al. Update of SMRI' s Compilation of Worldwide Salt Deposits and Salt Cavern Fields. 2018.

[17] Evans DJ, Chadwick RA. Underground Gas Storage Worldwide Experiences and Future Development in the UK and Europe. Evans DJ, Chadwick RA, editors. London: The Geological Society; 2009. 283 p.

[18] Czochal S. Dokumentacja geologiczna złoża wysadowego soli kamiennej Goleniów w kat. D w miejsc. Zielonczyn gm. Stepnica, Goleniów, woj. zachodniopomorskie. Nag Pig [271/2014]. Warszawa; 2013.

[19] Bünger U, Michalski J, Crotogino F, Kruck O. Large-scale underground storage of hydrogen for the grid integration of renewable energy and other applications. Compendium of Hydrogen Energy. Elsevier Ltd.; 2016. 133–163 p.

[20] Matos CR, Carneiro JF, Silva PP. Overview of Large-Scale Underground Energy Storage Technologies for Integration of Renewable Energies and Criteria for Reservoir Identification. J Energy Storage. 2019;21(November 2018):241–58.

[21] Khaledi K, Mahmoudi E, Datcheva M, Schanz T. Stability and serviceability of underground energy storage caverns in rock salt subjected to mechanical cyclic loading. Int J Rock Mech Min Sci. 2016;86:115–31.

[22] Liu W, Muhammad N, Chen J, Spiers CJ, Peach CJ, Deyi J, et al. Investigation on the permeability

characteristics of bedded salt rocks and the tightness of natural gas caverns in such formations. J Nat Gas Sci Eng. 2016;35:468–82.

[23] Wei L, Jie C, Deyi J, Xilin S, Yinping L, Daemen JJK, et al. Tightness and suitability evaluation of abandoned salt caverns served as hydrocarbon energies storage under adverse geological conditions (AGC). Appl Energy. 2016;178:703–20.

[24] Kunstman A, Urbańczyk K. Podziemne magazynowanie energii: wodór w kawernach solnych – aspekty ekonomiczne. Przegląd Solny / Salt Rev. 2013;9:20–5.

[25] Tarkowski R, Uliasz-Misiak B, Tarkowski P. Storage of hydrogen, natural gas, and carbon dioxide – Geological and legal conditions. Int J Hydrogen Energy. 2021;46(38):20010–22.

[26] Crotogino F, Schneider GS, Evans DJ. Renewable energy storage in geological formations. Proc Inst Mech Eng Part A J Power Energy. 2018;232(1):100–14.

[27] Pottier JD, Blondin E. Mass Storage of Hydrogen. In: Yurum Y, editor. Hydrogen Energy System, Utilization of Hydrogen and Future Aspects. Dordrecht: The Netherlands: Kluwer Academic Publishers; 1995. p. 167–79.

[28] Luboń K, Tarkowski R. Numerical simulation of hydrogen injection and withdrawal to and from a deep aquifer in NW Poland. Int J Hydrogen Energy. 2019;45:2068–83.

[29] Zivar D, Kumar S, Foroozesh J. Underground hydrogen storage: A comprehensive review. Int J Hydrogen Energy. 2021;46(45):23436–62.

[30] Crotogino F, Huebner S. Energy Storage in Salt Caverns. Developments and Concrete Projects for Adiabatic Compressed Air and for Hydrogen Storage. In: SMRI Spring 2008 Technical Conference. Porto: Solution Mining Research Institute; 2008. p. 1–12.

[31] Chapman A, Itaoka K, Hirose K, Davidson FT, Nagasawa K, Lloyd AC, et al. A review of four case studies assessing the potential for hydrogen penetration of the future energy system. Int J Hydrogen Energy. 2019;44(13):6371–82.

[32] Executive Summary of Assessment of the Potential, the Actors and Relevant Business Cases for Large Scale and Long Term Storage of Renewable Electricity by Hydrogen Underground Storage in Europe - Grant agreement no.: 303417. 2014.

[33] Simon J, Ferriz AM, Correas LC. HyUnder - Hydrogen underground storage at large scale: Case study Spain. Energy Procedia. 2015;73:136–44.

[34] Caglayan DG, Weber N, Heinrichs HU, Linßen J, Robinius M, Kukla PA, et al. Technical potential of salt caverns for hydrogen storage in Europe. Int J Hydrogen Energy. 2020;45(11):6793–805.

[35] Mouli-Castillo J, Heinemann N, Edlmann K. Mapping geological hydrogen storage capacity and regional heating demands: An applied UK case study. Appl Energy. 2021;283(December 2020):116348.

[36] Stone HBJ, Veldhuis IVO, Richardson RN. Underground hydrogen storage in the UK. Geol Soc London Spec Publ. 2009;313(1):217–26.

[37] Juez-Larré J, Gessel S Van, Dalman R, Remmelts G, Groenenberg R. Assessment of underground energy storage potential to support the energy transition in the Netherlands. First Break. 2019;37(7):57–66.

[38] Carneiro JF, Matos CR, Gessel S Van. Opportunities for large-scale energy storage in geological formations in mainland Portugal. Renew Sustain Energy Rev. 2019;99:201–11.

[39] Ozarslan A. Large-scale hydrogen energy storage in salt caverns. Int J Hydrogen Energy. 2012;37(19):14265–77.

[40] Lemieux A, Shkarupin A, Sharp K. Geologic feasibility of underground hydrogen storage in Canada. Int J Hydrogen Energy. 2020;45(56):32243–59.

[41] Qiu Y, Zhou S, Wang J, Chou J, Fang Y, Pan G, et al. Feasibility analysis of utilising underground hydrogen storage facilities in integrated energy system: Case studies in China. Appl Energy. 2020;269(February):115140.

[42] Czapowski G. Perspektywy lokowania kawern magazynowych wodoru w pokładowych wystąpieniach soli kamiennych górnego permu (cechsztyn) w Polsce – ocena geologiczna Prospects of Hydrogen Storage Caverns Location in the Upper Permian (Zechstein). Biul Państwowego Inst Geol. 2019;477:21–54.

[43] Ślizowski J, Urbańczyk K, Łaciak M, Lankof L, Serbin K. Efektywność magazynowania gazu ziemnego i wodoru w kawernach solnych. Effectiveness of natural gas and hydrogen storage in salt caverns. Przem Chem. 2017;96(5):994–8.

[44] Lankof L, Tarkowski R. Assessment of the potential for underground hydrogen storage in bedded salt formation. Int J Hydrogen Energy. 2020;45(38):19479–92.

[45] Wang T, Yan X, Yang H, Yang X, Jiang T, Zhao S. A new shape design method of salt cavern used as

underground gas storage. Appl Energy. 2013;104:50–61.

[46] Yee JK. Solution Mining Plan for the Enlargement of an Existing Storage Cavern Capacity with Additional Leaching Program at Mont Belvieu, Texas. In: SMRI Spring 2015 Technical Conference. Rochester: Solution Mining Research Institute; 2015.

[47] Cyran K. Insight Into a Shape of Salt Storage Caverns. Arch Min Sci. 2020;65(2):363–98.

[48] Cyran K, Kowalski M. Shape Modelling and Volume Optimisation of Salt Caverns for Energy Storage. Appl Sci. 2021;11(423):1–24.

[49] Ślizowski J, Lankof L, Wojtuszewska K. Geomechaniczna ocena optymalnej głębokości komór magazynowych gazu ziemnego w polskich złożach soli kamiennej. In: Materiały konferencji naukowej Warsztaty Górnicze z cyklu „Zagrożenia naturalne w górnictwie". Kraków: Instytut Gospodarki Surowcami Mineralnymi i Energią PAN; 2007. p. 423–31.

[50] Bérest P, Brouard B, Favret F, Hevin G, Karimi-Jafari M. Maximum Pressure in Gas Storage Caverns. In: SMRI Spring 2015 Technical Conference. Rochester; 2015. p. 17.

[51] Wang T, Li J, Jing G, Zhang Q, Yang C, Daemen JJK. Determination of the maximum allowable gas pressure for an underground gas storage salt cavern – A case study of Jintan, China. J Rock Mech Geotech Eng. 2019;11(2):251–62.

[52] Ślizowski J, Smulski R, Nagy S, Burliga S, Polański K. Tightness of Hydrogen Storage Caverns in Salt Deposits. AGH DRILLING, OIL, GAS. 2017;34(2):397–409.

[53] Pajak̨ L, Lankof L, Tomaszewska B, Wojnarowski P, Janiga D. The development of the temperature disturbance zone in the surrounding of a salt cavern caused by the leaching process for safety hydrogen storage. Energies. 2021;14(4).

[54] Zhu C, Arson C. A thermo-mechanical damage model for rock stiffness during anisotropic crack opening and closure. Acta Geotech. 2014;9(5):847–67.

[55] Pudewills A. Numerical simulation of coupled Thermo-Hydro-Mechanical processes in rock salt. In: Bérest P, Ghoreychi M, Hadj-Hassen F, Tijani M, editors. Mechanical Behaviour of Salt VII. CRC Press Taylor & Francis; 2012.

[56] Urbańczyk K. Wybrane aspekty termodynamiczne magazynowania wodoru w kawernach solnych. Przegląd Solny / Salt Rev. 2016;12:92–7.

[57] Passaris E, Jessop M, Slingsby J. Verification of the Salt Creep Parameters Using Data from the Echometric Surveys of Aldbrough Gas Storage Caverns in the UK. In: SMRI Spring 2015 Technical Conference. Rochester: Solution Mining Research Institute; 2015.

[58] Böttcher N, Görke UJ, Kolditz O, Nagel T. Thermo-mechanical investigation of salt caverns for short-term hydrogen storage. Environ Earth Sci. 2017;76(3).

[59] Wang T, Ao L, Wang B, Ding S, Wang K, Yao F, et al. Tightness of an underground energy storage salt cavern with adverse geological conditions. Energy. 2022;238:121906.

[60] Zhang G, Li Y, Yang C, Daemen JJK. Stability and tightness evaluation of bedded rock salt formations for underground gas/oil storage. Acta Geotech. 2014;9:161–79.

[61] Brouard B, Bérest P, Durup G. In - Situ Salt Permeability Testing. In: SMRI Fall 2001 Meeting. Albuquerque: Solution Mining Research Institute; 2001.

[62] Sørensen B. Underground Hydrogen Storage in Geological Formations, and Comparison With Other Storage Solutions. In: Hydrogen Power Theoretical and Engineering Int Symp. 2007. p. 9.

[63] Amro M, Häfner F, Freese C. Modern In situ and Laboratory Measurements of Permeability and Porosity to Prove Tightness of Underground Storage of Hydrogen, Natural Gas and CO2. In: SMRI Fall 2012 Technical Conference. Bremen; 2012.

[64] Abuaisha M, Billiotte J. A discussion on hydrogen migration in rock salt for tight underground storage with an insight into a laboratory setup. J Energy Storage. 2021;38(April):102589.

[65] Audigane P, Gentier S, Bader A-G, Beccaletto L, Bellenfant G. The role of the underground for massive storage of energy: a preliminary glance of the French case. Geophys Res Abstr. 2014;16:12555.

[66] Hemme C, van Berk W. Potential risk of H2S generation and release in salt cavern gas storage. J Nat Gas Sci Eng. 2017;47:114–23.

[67] Schlichtenmayer M, Bannach A, Amro M, Freese C. Renewable Energy Storage in Salt Caverns - A Comparison of Thermodynamics and Permeability between Natural Gas, Air and Hydrogen. 2015.

[68] Ślizowski J, Urbańczyk K, Czapowski G, Lankof L, Serbin K, Ślizowski K, et al. Możliwości magazynowania gazu ziemnego w polskich złożach soli kamiennej w zależności od warunków geologiczno-górniczych. Ślizowski J, Urbańczyk K, editors. Kraków: Wydawnictwo IGSMiE PAN; 2011. 132 p.

[69] Zapf D. Rock Mechanical Dimensioning of Gas Storage Caverns in the Salt Dome Edge Region. In: SMRI Fall 2014 Technical Conference. Groningen; 2014. p. 855–62.

[70] Wang T, Yang C, Ma H, Li Y, Shi X, Li J, et al. Safety evaluation of salt cavern gas storage close to an old cavern. Int J Rock Mech Min Sci. 2016;83:95–106.

[71] Bérest P, Brouard B. A tentative classification of salts according to their creep properties. In: SMRI Spring 1998 Meeting. New Orleans: Solution Mining Research Institute; 1998. p. 1–21.

[72] Gąska K, Hoszowski A, Gmiński Z, Kurek A. Monografia Podziemnych Magazynów Gazu. Warszawa: Oficyna Wydawnicza ASPRA-JR; 2012.

[73] Ślizowski K. Warunki geologiczno-górnicze w cechsztyńskich złożach soli w Polsce dla wykonywania podziemnych zbiorników cieczy i gazu. Zesz Nauk AGH, Górnictwo. 1983;(121).

[74] Wang T, Ma HL, Shi XL, Yang CH, Zhang N, Li JL, et al. Salt cavern gas storage in an ultra-deep formation in Hubei, China. Int J Rock Mech Min Sci. 2018;102:47–70.

[75] Serbin K, Ślizowski J, Urbańczyk K, Nagy S. The influence of thermodynamic effects on gas storage cavern convergence. Int J Rock Mech Min Sci. 2015;79:166–71.

[76] Li W, Miao X, Yang C. Failure analysis for gas storage salt cavern by thermo-mechanical modelling considering rock salt creep. J Energy Storage. 2020;32(August):102004.

[77] Ślizowski J, Lankof L, Urbańczyk K, Serbin K. Potential capacity of gas storage caverns in rock salt bedded deposits in Poland. J Nat Gas Sci Eng. 2017 Jul;43:167–78.

[78] Mahmoudi E, Khaledi K, Miro S, Konig D, Schanz T. Probabilistic Analysis of a Rock Salt Cavern with Application to Energy Storage Systems. Rock Mech Rock Eng. 2017;l(50):139–57.

[79] Yang C, Wang T, Li J, Ma H, Shi X, Daemen JJK. Feasibility analysis of using closely spaced caverns in bedded rock salt for underground gas storage: a case study. Environ Earth Sci. 2016;75(15):1–15.

[80] Ghoreychi M, Daupley X, Laouafa F. Creep and damage impact on long-term stability of underground structures in salt formations. In: Bérest P, Ghoreychi M, Hadj-Hassen F, Tijani M, editors. Mechanical Behavior of Salt VII Proceedings of the 7th Conference on the Mechanical Behavior of Salt. CRC Press Taylor & Francis, 2012; 2012.

[81] Song R, Yue-Ming B, De-Yi J, Xiao-Yong L. Study on the comprehensive evaluation model for the stability of the bedded salt rock gas storage during the operation period. In: Bérest P, Ghoreychi M,

Hadj-Hassen F, editors. Mechanical Behavior of Salt VII Proceedings of the 7th Conference on the Mechanical Behavior of Salt. CRC Press Taylor & Francis; 2012.

[82] Tarkowski R, Uliasz-Misiak B. Use of underground space for the storage of selected gases (CH4, H2, and CO2) – possible conflicts of interest. Gospod Surowcami Miner / Miner Resour Manag. 2021;37(1):141–60.

[83] Hadj-Hassen F, Tijani M, Rouabhi A, Hertz E. Interpretation of convergence movement in room and pillar mining by integrating creep of salt and swelling of marl under water effect. In: Bérest P, Ghoreychi M, Hadj-Hassen F, Tijani M, editors. Mechanical Behavior of Salt VII Proceedings of the 7th Conference on the Mechanical Behavior of Salt. 2012. p. 201–8.

[84] Tijani M, Hadj-Hassen F, Rouabhi A, Schleifer J, Gatelier N. Effect of insoluble materials on salt behavior during creep tests. In: Bérest P, Ghoreychi M, Hadj-Hassen F, Tijani M, editors. Proceedings of the 7th Conference on the Mechanical Behavior of Salt. Paris: CRC Press Taylor & Francis; 2012.

[85] Van Sambeek LL. Measurements of humidity-enhanced salt creep in salt mines: Proving the Joffe effect. In: Bérest P, Ghoreychi M, Hadj-Hassen F, Tijani M, editors. Mechanical Behavior of Salt VII Proceedings of the 7th Conference on the Mechanical Behavior of Salt. 2012. p. 179–84.

[86] Wang L, Bérest P, Brouard B. Mechanical Behavior of Salt Caverns: Closed-Form Solutions vs Numerical Computations. Rock Mech Rock Eng. 2015;48(6):2369–82.

[87] Ma X, Xu Z, Chen L, Shi X. Creep deformation analysis of gas storage in salt caverns. Int J Rock Mech Min Sci. 2021;139(October 2020):104635.

[88] Liang G, Huang X, Peng X, Tian Y, Yu Y. Investigation on the cavity evolution of underground salt cavern gas storages. J Nat Gas Sci Eng. 2016;33:118–34.

[89] IEA, Global hydrogen demand by sector in the Net Zero Scenario, 2020-2030, IEA, Paris [Internet]. [cited 2022 Feb 7]. Available from: https://www.iea.org/data-and-statistics/charts/global-hydrogen-demand-by-sector-in-the-net-zero-scenario-2020-2030.